AD-A183 827 A PRELIMINARY ANALYSIS OF SEISMIC VARIABILITY AT THE SHAGGAN RIVER NUCLEAR TEST SITE(U) S-CUBED LA JOLLA CA J H DERMENGIAN ET AL. DEC 85 SSS-R-87-7500 AC4MC107 1/1

UNCLASSIFIED F/G 17/10 NL

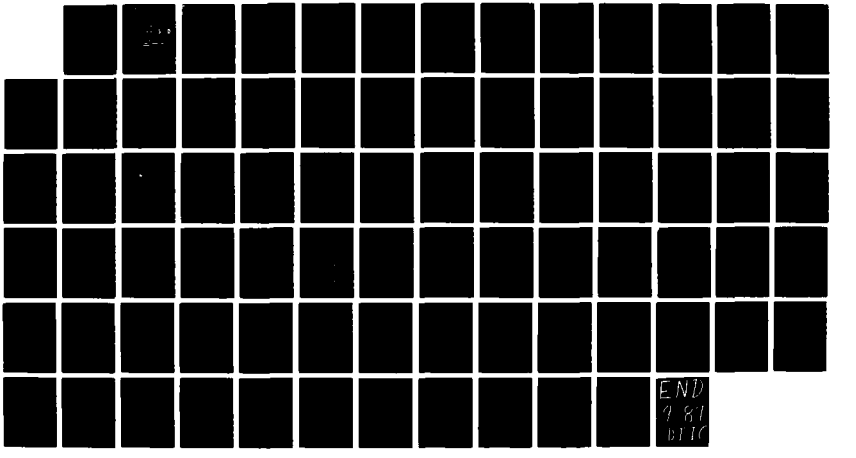

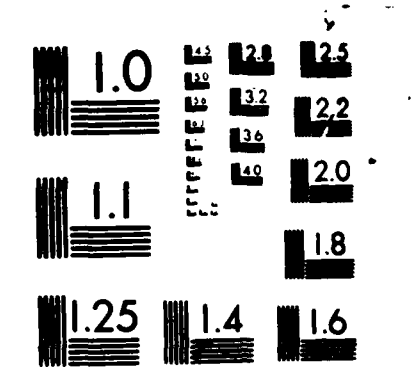

S-CUBED
A Division of Maxwell Laboratories, Inc.

SSS-R-86-7580

A PRELIMINARY ANALYSIS OF SEISMIC VARIABILITY AT THE SHAGAN RIVER NUCLEAR TEST SITE

J. M. DERMENGIAN
J. R. MURPHY
B. W. BARKER

FINAL REPORT

PREPARED FOR:

U. S. ARMS CONTROL AND DISARMAMENT AGENCY
WASHINGTON, D. C. 20451

CONTRACT NO. AC4MC107

DECEMBER 1985

P. O. Box 1620, La Jolla, California 92038-1620
(619) 453-0060

REPORT DOCUMENTATION PAGE	1. REPORT NO. AD-A183827	2. Recipient's Accession No.
4. Title and Subtitle A PRELIMINARY ANALYSIS OF SEISMIC VARIABILITY AT THE SHAGAN RIVER NUCLEAR TEST SITE		5. Report Date December 1985 6.
7. Author(s) J.M. Dermengian, J.R. Murphy, and B.W. Barker		8. Performing Organization Rept. No. SSS-R-86-7580
9. Performing Organization Name and Address S-CUBED Division of Maxwell Laboratories, Inc. P. O. Box 1620 La Jolla, California 92038-1620		10. Project/Task/Work Unit No. 11. Contract(C) or Grant(G) No. (C) AC4MC107 (G)
12. Sponsoring Organization Name and Address United States Arms Control and Disarmament Agency Washington, D.C. 20451		13. Type of Report & Period Covered Final Report 14.

15. Supplementary Notes

16. Abstract (Limit: 200 words)

The research investigation described in this report has focused on a preliminary analysis of seismic variability at the Shagan River nuclear test site. In order to carry out this analysis, large volumes of teleseismic P wave amplitude and arrival time data recorded from explosions at this test site were collected and statistically analyzed in an attempt to define any systematic trends which correlate with source location. The results of the analysis of the teleseismic m_b data have been shown to provide strong evidence of systematic geophysical variations within the Shagan River testing area. In particular, the m_b station corrections have been shown to vary with source location in a manner which depends on source-to-station azimuth. Results of detailed comparisons of m_b residual data at common stations from selected pairs of nearby explosions have been used to conclude that the observed variations in the azimuthal patterns of the m_b residuals are related to event location rather than tectonic release effects. In fact the results of this preliminary analysis suggest that the observed m_b differences may be associated with changes in the near-source portions of the teleseismic P wave propagation paths.

In contrast to the m_b residual data, the reduced P wave travel-time residuals were found to show no obvious correlation with event location, and this has been interpreted as an indication that the available bulletin data are not precise enough to resolve the rather small travel-time variations which might be expected to accompany the observed m_b variations.

17. Document Analysis a. Descriptors

Underground Nuclear Explosions
Seismic Detection
Numerical Analysis

b. Identifiers/Open-Ended Terms

Teleseismic P Waves
Geophysically Distinct
Least Squares Matrix Factorization
m_b Residuals
Travel-Time Residuals
Tectonic Release
Test Site Variability
Shagan River

c. COSATI Field/Group

18. Availability Statement: RELEASE unlimited	19. Security Class (This Report) UNCLASSIFIED	21. No. of Pages
	20. Security Class (This Page) UNCLASSIFIED	22. Price

TABLE OF CONTENTS

LIST OF ILLUSTRATIONS

LIST OF ILLUSTRATIONS (Cont'd)

LIST OF ILLUSTRATIONS (Cont'd)

LIST OF TABLES

EXECUTIVE SUMMARY

This report summarizes the results of a preliminary investigation of seismic variability within the Shagan River region of the Russian nuclear test site at Semipalatinsk. The primary objective of this study has been to assess the feasibility of using teleseismic P wave amplitude and arrival time data recorded from explosions at this test site to define any systematic trends which correlate with source location.

The teleseismic P wave data base which has been assembled for this purpose is described in Section II where the distributions of the data with respect to source and station parameters are documented in detail. These data consist of individual m_b readings and P wave arrival times recorded by a selected network of 94 worldwide receiver stations from a sample of 52 Shagan River underground nuclear explosions which have been assigned m_b values of 5.5 or greater. These seismic data, together with the refined explosion epicenters and origin times determined by Marshall et al. (1984), have provided the basis for investigating test site variability.

Standard seismological and statistical procedures are applied to these data in Section III where network-averaged magnitudes are computed for each explosion and average m_b correction factors are determined for each of the selected stations which recorded these events. The variations of these m_b station correction factors with source location are then carefully analyzed and shown to strongly support the conclusion that systematic geophysical variations occur within the Shagan River testing area. In particular, it is demonstrated that the corrected, single station m_b residuals for explosions in the southwest portion of the test site appear to be random at any given azimuth and

quite similar from event to event, while there are large (0.5 units m_b) variations in the corrected m_b residuals with azimuth between explosions in close proximity in the northeast and central portions of the test site. Detailed comparisons of m_b residual data from selected pairs of explosions are then used to demonstrate that the observed variations in the azimuthal patterns of these residuals are related to event location rather than tectonic release effects. Moreover, results of some preliminary analyses are presented which suggest that the variations in the m_b corrections for stations in a given azimuth are systematic enough to be contoured as a function of source location. This is interpreted as an indication that the observed differences are associated with changes in the near-source P wave propagation paths to teleseismic distances as a function of source location within the test site.

The results of some preliminary analyses of the P wave travel-time data are also presented in Section III where it is shown that the reduced P wave travel-time residuals do not show the correlation with event location inferred from the analysis of the corresponding m_b residual data. These results are interpreted as an indication that the ISC travel time data are not precise enough to be useful for identifying variations in the subsurface geology across the Shagan River test site.

I. INTRODUCTION

In 1974, the U.S. and U.S.S.R. signed a Threshold Test Ban Treaty (TTBT) which prohibits the testing of underground nuclear explosions with yields greater than 150 kilotons. Upon ratification, the treaty calls for the bilateral exchange of certain geologic and geophysical data, as well as the yields of two calibration events, in each so-called "geophysically distinct" testing area, in order to facilitate verification of treaty compliance. Although not defined explicitly in the TTBT protocol, the term "geophysically distinct" is intended to denote an area within which the geophysical properties controlling the magnitude-yield relationship are uniform - that is, an area within which a single yield-scaling relation holds for all explosions. Given adequate calibration data, such areas are generally fairly easy to recognize. For example, at the Nevada Test Site (NTS), the differences between the seismic coupling characteristics of explosions in the dry alluvium environment of Yucca Flat versus those in the saturated volcanic environment of Pahute Mesa are easily recognized by comparing the magnitude-yield populations characteristic of those two testing areas. However, for areas such as the Semipalatinsk test site in the U.S.S.R., for which such calibration data are not available, it is not obvious how such geophysically distinct areas could be identified using information known to us at the present time. The objective of the preliminary research investigation described in this report has been to assess the feasibility of using teleseismic P wave data recorded from explosions to identify geophysically distinct testing areas within the Shagan River region of the Semipalatinsk test site.

Figure 1 shows the geographic location of the principal Russian Nuclear Testing Ground (NTG) near Semipalatinsk

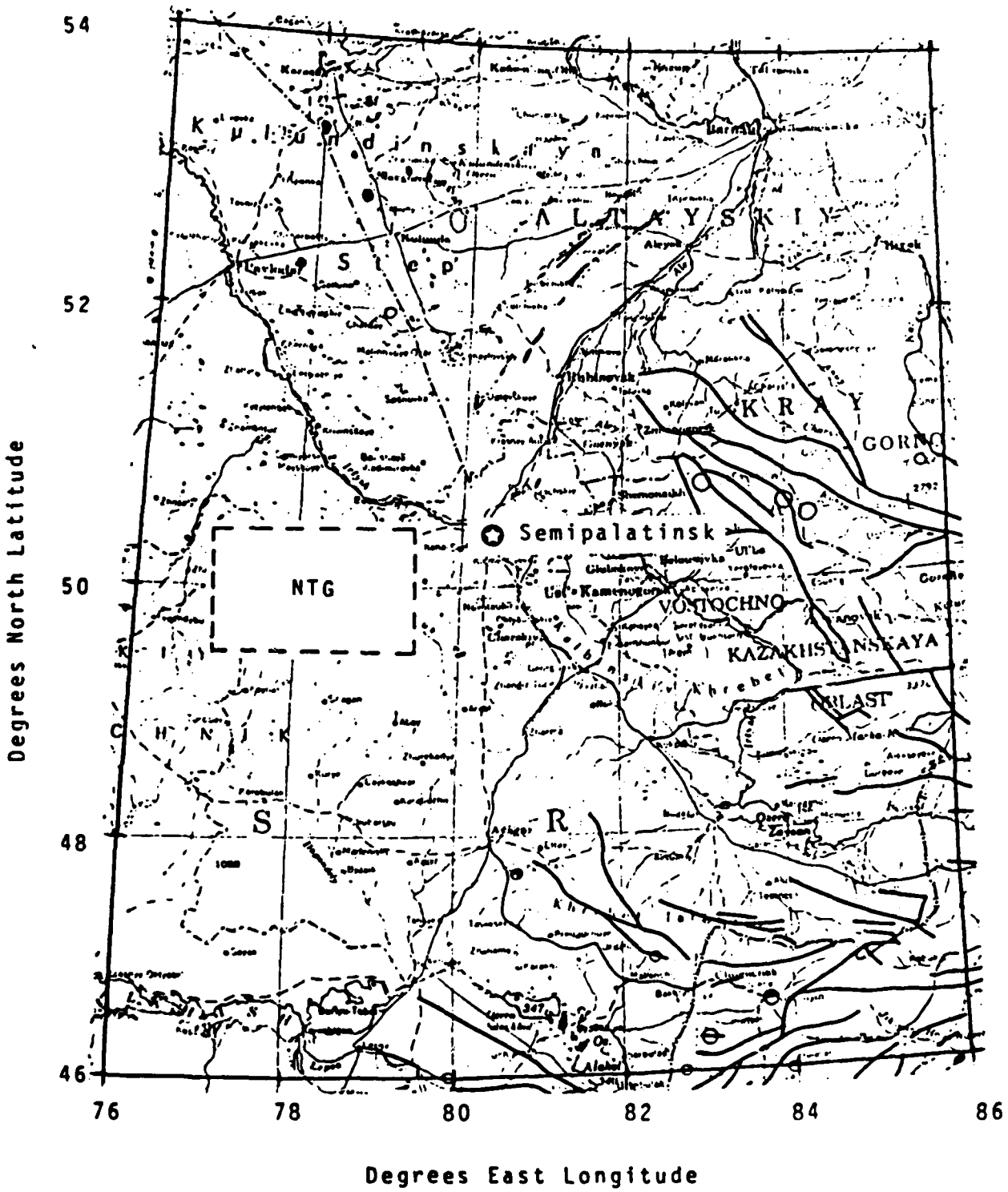

Figure 1. Geographic map of Eastern Kazakhstan Province, U.S.S.R., showing the city of Semipalatinsk (✪) and the approximate location of the Nuclear Testing Ground (NTG).

in the Eastern Kazakhstan Province of the U.S.S.R. It can be seen that the NTG is quite large, covering a total surface area of approximately 36,000 km^2. However, most of the underground nuclear testing conducted at this site occurs in two restricted areas known as the Degelen Mountain and Shagan River testing areas. These two sites are outlined in Figure 2 where it can be seen that the Degelen test site is located in the central part of the NTG and occupies a surface area of approximately 410 km^2 while the larger Shagan River test site is located in the northeast quadrant of the NTG and occupies a surface area of approximately 640 km^2. In recent years, the largest magnitude Russian underground nuclear explosions have consistently occurred at the Shagan River test site and, consequently, it is this area which is currently of primary interest with regard to yield estimation. The contours superimposed on the maps in Figure 2 denote the variations in crust and upper mantle structure across the area as inferred from Russian gravity and magnetic data (Zlavdinov, 1974). It can be seen that these data suggest some systematic variations in crustal structure across the NTG. Thus, for example, in the vicinity of the Degelen site the sedimentary cover is virtually absent, the granitic layer has an average thickness of 20 km, the basaltic layer has a maximum thickness of 21 km and the depth to the Moho is as great as 41 km; while at the Shagan River site the sedimentary layer thickens to as much as 7 km, the granitic and basaltic layers both decrease in thickness (to 13 km and 18.5 km respectively) and the average Moho depth is about 39 km. It is reasonable to expect that these large scale crustal variations may be associated with smaller scale variations in structure at the shallower depths where testing is taking place, and it is these latter variations which we will be attempting to map through comparisons of the teleseismic P waves recorded from various Shagan River

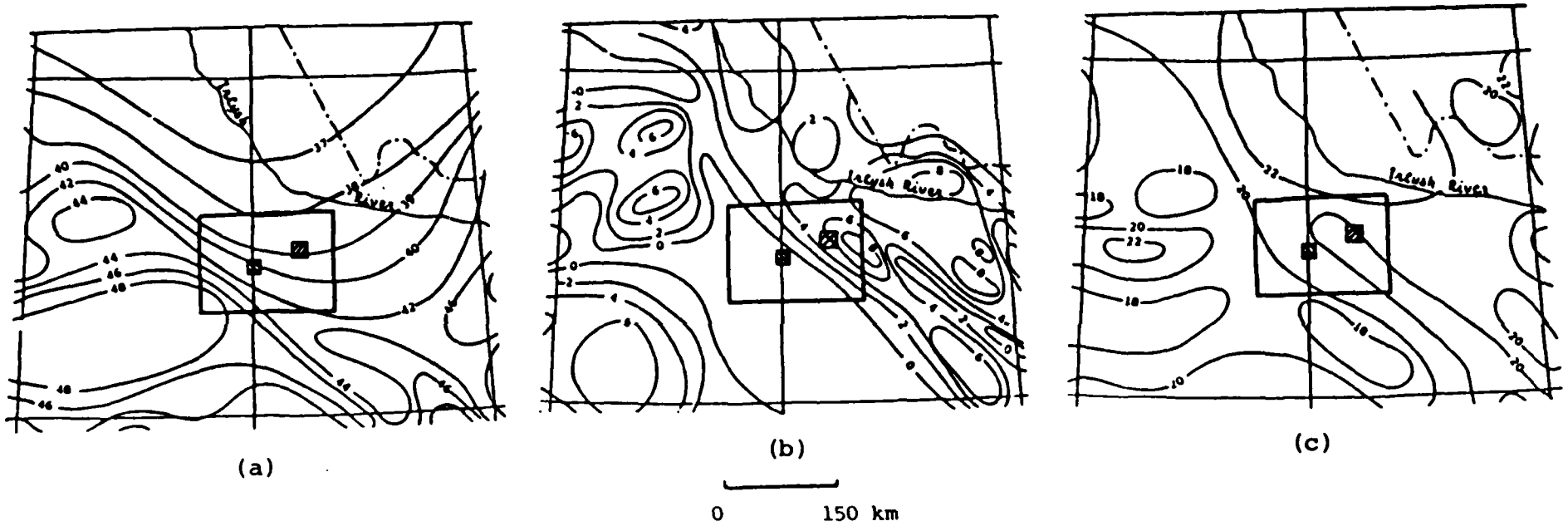

Figure 2. Contour maps of crust and upper mantle structure in Semipalatinsk area, Eastern Kazakhstan. (a) Depth (in km) of Moho, (b) depth (in km) to top of granitic layer, and (c) depth (in km) to top of basaltic layer. The Nuclear Testing Ground (NTG) is outlined in box; Shagan River (eastern) test site denoted by NE-SW hatched pattern and Degelen Mtn. (central) test site denoted by NW-SE hatched pattern. (Adapted from Zlavdinov, 1974).

underground explosions.

The organization of this report may be briefly summarized as follows. The data samples of teleseismic P wave amplitudes and travel times compiled for the purposes of this study are described in detail in Section II. In Section III these data are analyzed using a variety of statistical analysis techniques in an attempt to isolate any significant correlations with event location. This is followed in Section IV by a summary and a listing of preliminary conclusions concerning variations in teleseismic P wave characteristics with source location within the Shagan River test site.

II. DESCRIPTION OF THE TELESEISMIC P WAVE DATA BASE

The data sample which has been compiled to investigate variability at the Shagan River test site is composed of teleseismic P wave observations recorded from underground nuclear explosions conducted at that site. In assembling this sample, only those explosions which occurred in the time interval 1964 through 1982 which have been assigned m_b values of greater than 5.5 by ISC have been considered. This time interval was selected to coincide with that for which data are available from either the ISC Bulletins or the NEIS Earthquake Data Reports, while the m_b threshold of 5.5 was adopted to guarantee reasonably uniform recording by the worldwide networks of stations. Using these criteria, a sample of 52 Shagan River explosions has been identified for analysis. The ISC source parameters for these 52 explosions are listed in Table 1, together with the epicenter locations obtained for these same events by Marshall et al. (1984) using the Joint Epicenter Determination (JED) method. These latter locations are believed to be considerably more accurate in that they have been computed relative to the known location of the Shagan River cratering explosion of 1/15/65 (event # 1 in Table 1) and, consequently, will be used for the purposes of this investigation. The JED locations of the 52 explosions of Table 1 are displayed graphically in Figure 3 where it can be seen that they are fairly broadly distributed across the Shagan River testing area. The 95 percent confidence ellipses about these epicenters reported by Marshall et al. (1984) suggest that these locations are accurate to within a few kilometers in most cases. The distribution of these events with respect to ISC m_b value is shown in Figure 4 where it can be seen that the majority of the explosions have been assigned m_b values in the range

Table 1

SHAGAN RIVER EXPLOSION SAMPLE

Event No.	Date M D Y	ISC Origin Time Hr Min Sec	Location (°N Lat., °E Long.) ISC	JED	ISC m_b (Number of Stations)
01	01/15/65	05 59 58.4	49.88 78.96	49.940 79.010†	5.8 (11)
02	11/30/69	03 32 57.3	49.94 78.98	49.913 78.961	6.0 (65)
03	11/02/72	01 26 57.8	49.91 78.85	49.923 78.815	6.1 (75)
04	12/10/72	04 27 07.6	49.97 78.95	50.001 78.973	6.0 (26)
05	07/23/73	01 22 57.7	49.94 78.85	49.962 78.812	6.1 (81)
06	12/14/73	07 46 57.1	50.03 79.02	50.044 78.987	5.8 (67)
07	05/31/74	03 26 57.4	49.91 78.91	49.950 78.852	5.9 (83)
08	10/16/74	06 32 57.6	49.99 78.96	49.979 78.898	5.5 (63)
09	12/27/74	05 46 56.8	49.91 79.05	49.943 79.011	5.6 (60)
10	04/27/75	05 36 57.2	49.94 79.02	49.949 78.926	5.6 (71)
11	10/29/75	04 46 57.3	49.92 78.91	49.946 78.878	5.8 (64)
12	12/25/75	05 16 57.2	50.02 78.86	50.044 78.814	5.7 (70)
13	07/04/76	02 56 57.5	49.85 78.97	49.909 78.911	5.8 (83)
14	08/28/76	02 56 57.6	49.95 78.98	49.969 78.930	5.8 (82)
15	11/23/76	05 02 57.5	49.97 79.01	50.008 78.963	5.8 (93)
16	12/07/76	04 56 57.5	49.87 78.89	49.922 78.846	5.9 (76)
17	05/29/77	02 56 57.5	49.86 78.84	49.937 78.770	5.8 (97)
18	09/05/77	03 02 57.8	50.05 78.93	50.035 78.921	5.8 (97)

Table 1 (Cont'd)

Event No.	Date M D Y	ISC Origin Time Hr Min Sec	Location(°N Lat.,°E Long.) ISC	JED	ISC m_b(Number of Stations)
19	10/29/77	03 07 02.9	50.06 78.87	50.069 78.975	5.6 (53)
20	11/30/77	04 06 57.5	49.93 78.89	49.958 78.885	6.0 (90)
21	06/11/78	02 56 57.7	49.88 78.81	49.898 78.797	5.9 (92)
22	07/05/78	02 46 57.3	49.84 78.91	49.887 78.871	5.8 (96)
23	08/29/78	02 37 06.5	49.98 79.02	50.000 78.978	5.9 (80)
24	09/15/78	02 36 57.3	49.91 78.94	49.916 78.879	6.0 (100)
25	11/04/78	05 05 57.5	50.03 78.98	50.034 78.943	5.6 (106)
26	11/29/78	04 33 02.9	49.93 78.77	49.949 78.798	6.0 (82)
27	06/23/79	02 56 59.0	49.89 78.92	49.903 78.855	6.2 (121)
28	07/07/79	03 46 57.5	50.05 79.06	50.026 78.991	5.8 (109)
29	08/04/79	03 56 57.3	49.86 78.94	49.894 78.904	6.1 (137)
30	08/18/79	02 51 57.3	49.93 78.98	49.943 78.938	6.1 (135)
31	10/28/79	03 16 57.0	49.96 79.07	49.973 78.997	6.0 (127)
32	12/02/79	04 36 57.6	49.88 78.84	49.891 78.786	6.0 (118)
33	12/23/79	04 56 57.6	49.93 78.80	49.916 78.755	6.2 (116)
34	04/25/80	03 56 57.4	49.92 78.81	49.973 78.755	5.5 (103)
35	06/12/80	03 26 57.7	49.95 79.05	49.980 79.001	5.6 (91)
36	06/29/80	02 32 57.8	49.91 78.86	49.939 78.815	5.7 (88)
37	09/14/80	02 42 39.3	49.94 78.86	49.921 78.802	6.2 (104)
38	10/12/80	03 34 14.3	49.94 79.10	49.961 79.028	5.9 (118)

Table 1 (Cont'd)

Event No.	Date M D Y	ISC Origin Time Hr Min Sec	Location (°N Lat., °E Long.) ISC	JED	ISC m_b (Number of Stations
39	12/14/80	03 47 06.5	49.87 78.97	49.899 78.938	5.9 (115)
40	12/27/80	04 09 08.5	50.01 79.03	50.057 78.981	5.9 (90)
41	03/29/81	04 03 50.1	49.98 79.02	50.007 78.982	5.6 (105)
42	04/22/81	01 17 11.4	49.87 78.90	49.885 78.810	6.0 (127)
43	05/27/81	03 58 12.3	49.94 79.01	49.985 78.980	5.5 (93)
44	09/13/81	02 17 18.4	49.89 78.98	49.910 78.915	6.1 (131)
45	10/18/81	03 57 02.7	49.88 78.89	49.923 78.859	6.1 (111)
46	11/29/81	03 35 08.8	49.85 78.85	49.887 78.860	5.7 (109)
47	12/27/81	03 43 14.2	49.90 78.86	49.923 78.795	6.2 (128)
48	04/25/82	03 23 05.5	49.87 78.92	49.903 78.913	6.1 (121)
49	07/04/82	01 17 14.5	49.97 78.86	49.960 78.807	6.1 (114)
50	08/31/82	01 31 00.7	49.91 78.79	49.924 78.761	5.4 (78)*
51	12/05/82	03 37 12.7	49.93 78.87	49.919 78.813	6.1 (118)*
52	12/26/82	03 35 14.2	50.07 79.04	50.071 78.988	5.7 (98)*

† JED restrained hypocenter.

* The event parameters of explosions occurring since 08/31/82 onwards are those reported by the NEIS service.

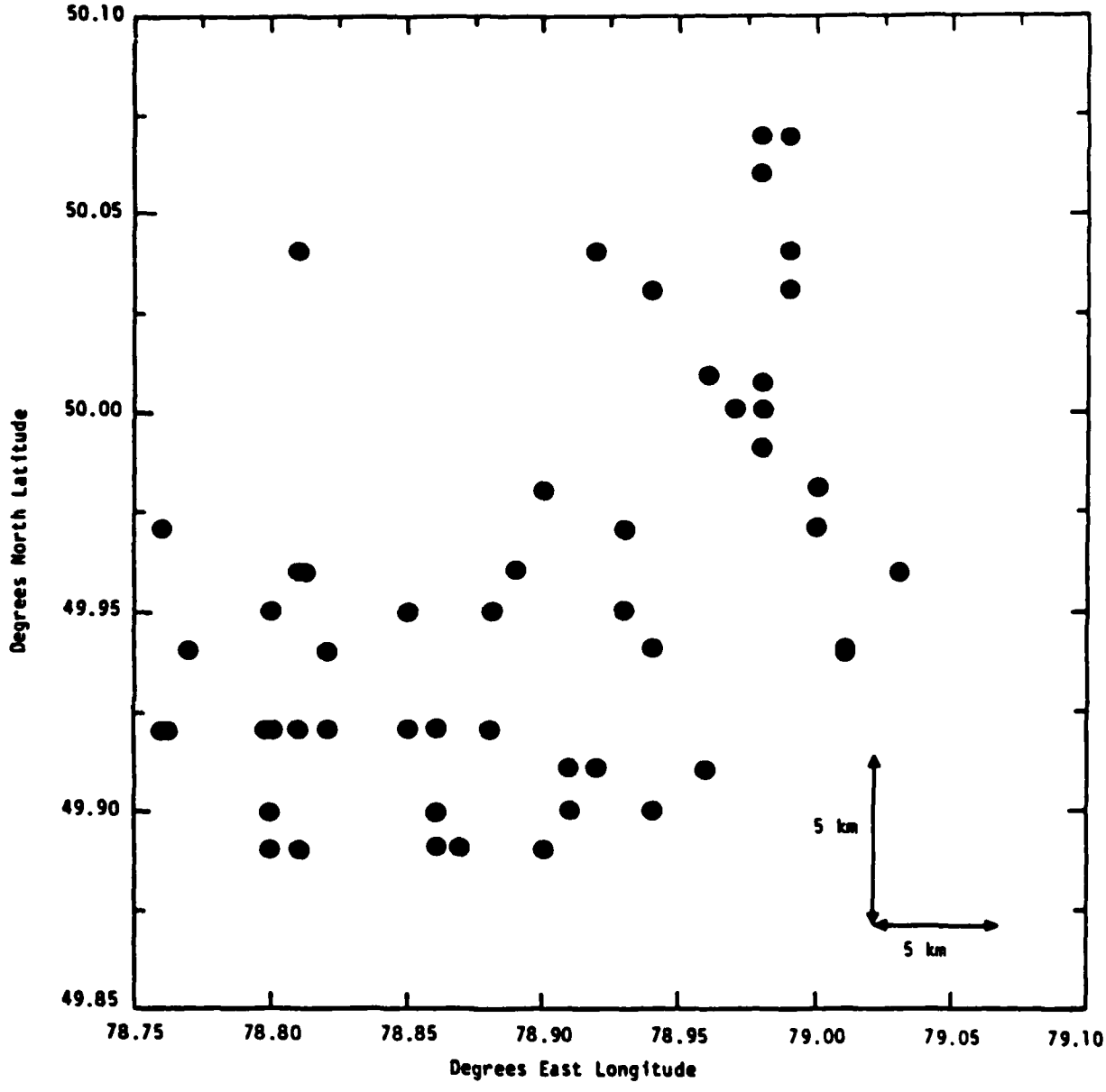

Figure 3. Map showing the JED relocations of Shagan River explosions used in this study.

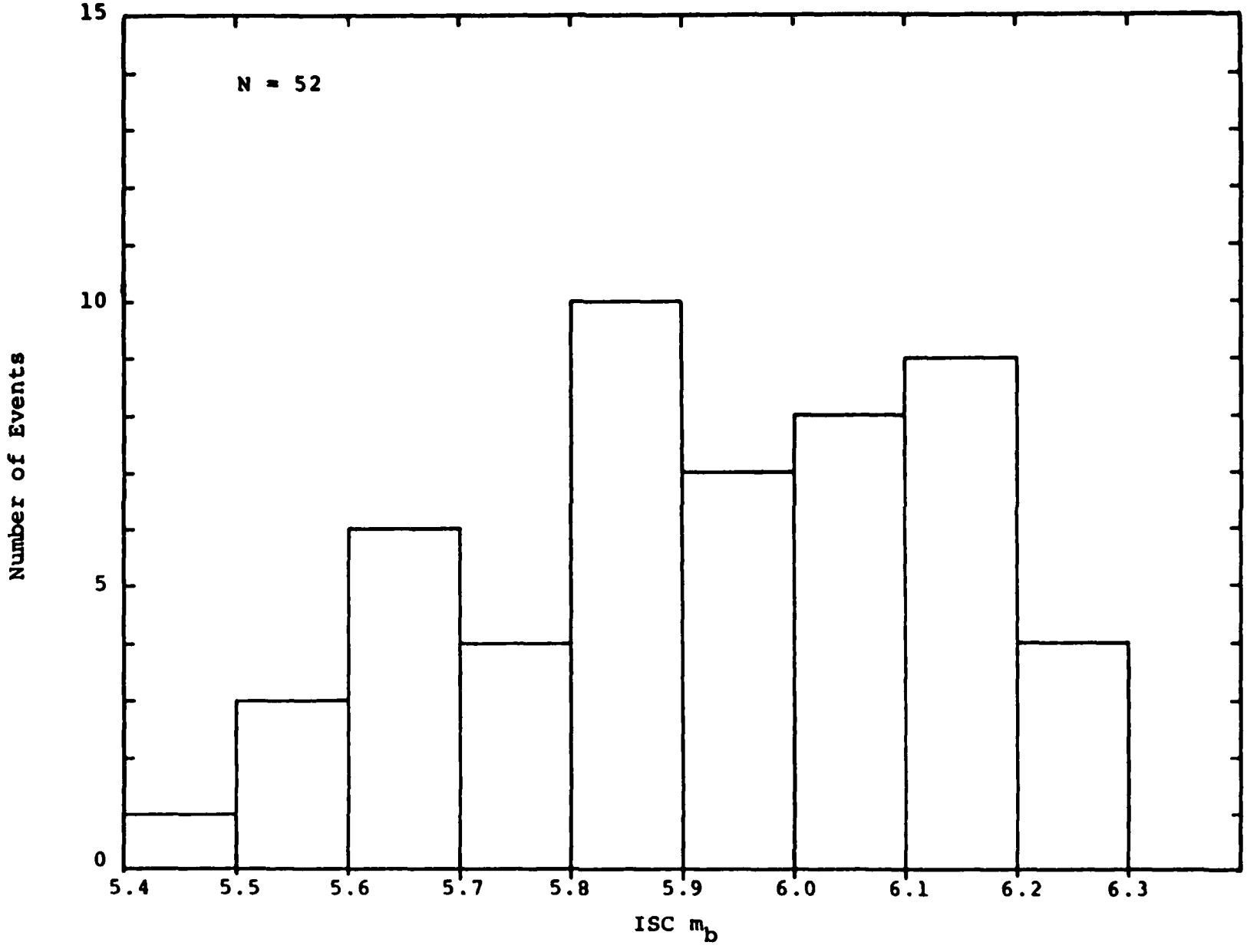

Figure 4. Frequency distribution of Shagan River explosion sample as a function of ISC m_b.

$5.6 \leq m_b \leq 6.2$, which is well within the optimum operating range of the worldwide seismic networks which report to ISC. At the present time, the source parameters for all events occurring since 8/31/82 are available from the NEIS service only; NEIS m_b values differ, on average, by 0.10 m_b units or less from ISC m_b values for this source region.

We have extracted all available teleseismic P wave observations for each selected explosion from earthquake catalogs published by the ISC and NEIS services. Over the time period encompassing our explosion sample (i.e., 1964 through 1982), a total of approximately 863 different worldwide seismic stations and arrays, ranging in epicentral distance from 30° to 105° and widely distributed in azimuth, reported teleseismic P wave detections from some of the selected 52 Shagan events. Of course, many of the 863 worldwide receiver stations were operational only within specific time periods and, thus, the reporting consistency varies significantly between stations. Our aim in defining an optimum data base has been to preserve the maximum number of common teleseismic stations, with both wide azimuthal and epicentral distance coverage, having detected all or most of the selected Shagan River explosions and reported all available event parameters. The event parameters that are most useful for our statistical analyses are P wave arrival time, travel time residual computed with respect to the travel time expected for a given distance in a standard, average earth model and individual station m_b, or the log of the ratio of P wave amplitude to period (i.e., log A/T). Every station detecting a given explosion in the event sample has reported at least P wave arrival time information allowing for the determination of travel time; therefore, the detection criteria for the selection of a suitable network of stations used in this study has been based primarily on observed arrival time data. As such, we have found that the

meaningful station coverage consists of 94 worldwide stations having detected at least 75 percent of the total explosion sample. The mean detection level for this group of stations is, however, 87 percent. There appears to be no significant advantage to selecting a detection level higher or lower than 75 percent since there is at least a 25 percent decrease in the station sample if the event detection level is constrained to 80 percent or higher; and, although a large increase (38 percent) in the total station sample is achieved by reducing the detection requirement to 65 percent, there is no net gain in the range of recording azimuths.

Unfortunately, due to inconsistency in station reporting, the number of stations for which individual station m_b data are available is frequently significantly smaller than the total number reporting arrival time data. By merging station data published in both ISC and NEIS catalogs, it has been possible to extract the maximum number of station m_b (or log A/T) values. Of the final 94 stations, 78 (i.e., 83 percent) have reported m_b (or log A/T) values for the Shagan explosion sample. The mean number of m_b (or log A/T) data available for this group is 27 ± 3 out of a possible 52 events, or 52 percent of the entire explosion sample. The statistical significance of the size of this m_b data base, relative to the size of the travel time data base, will be addressed in Section III. In cases where log A/T quantities have been reported, m_b values were calculated based on the appropriate Gutenberg-Richter distance correction factors. As a result of the above descriptions of the complete data base utilized in this study, we find that for our selected seismic network of 94 stations there are, on the average, 82 stations (or a range of 31 to 94) with travel time information and 41 stations (or a range of 15 to 59) with individual station m_b (or log A/T) values reported per event. To ensure effective statistical and seismological analyses, we

have compiled these data consisting of several thousand individual station arrival time and m_b values, carefully verified and assembled into a tractable data base on the DARPA Center for Seismic Studies (CSS) computer system in Rosslyn, Virginia.

The individual station information that is pertinent to this investigation, including epicentral distance and recording azimuth to the center of the Shagan test site, as well as number of event recordings available, are listed in Table 2. Figure 5 shows the azimuthal distribution of the teleseismic station coverage common to the Shagan explosion sample where it can be seen that, although there is generally wide azimuthal coverage, the predominant coverage occurs in the west-northwest and north-northeast azimuthal sectors. The distribution of these same stations on the basis of epicentral distance to the Shagan test site is displayed in Figure 6 indicating that the majority of stations are between 30 and 60 degrees away from Shagan. The actual map locations of the stations are shown on an azimuthally equidistant projection centered on the Shagan River test site in Figure 7, where it can be seen that the heaviest concentration of stations occurs in western Europe.

Table 2

TELESEISMIC STATION INFORMATION

Station Code	Δ°	AZ°	Number of Event Detections	
			m_b (or log A/T)	P-Wave Arrival Time
ADK	60.1	44	5	44
AKU	48.6	327	28	46
ALE	46.4	353	35	41
ALQ	95.4	4	31	52
ASP	88.0	131	21	44
BER	41.1	314	1	47
BKS	90.6	17	36	48
BRG	40.2	297	45	48
BSF	45.8	297	32	48
BUD	38.7	290	32	40
BUL	82.7	227	32	51
CDF	45.2	297	32	50
CHG	35.0	145	24	41
CLL	40.5	298	48	52
COL	59.9	21	25	45
COP	39.2	305	44	47
CTA	91.5	120	25	47
DAG	43.8	341	37	45
DOU	45.8	300	5	52
EDM	76.7	8	31	42
EKA	47.4	310	33	48
EUR	90.1	11	26	43
FFC	75.8	1	31	41
FHC	87.4	17	0	41
FLN	49.4	301	24	47
FRI	91.9	15	0	48
FUR	43.0	295	34	50

Table 2 (Cont'd)

Station Code	Δ°	AZ°	Number of Event Detections: m_b (or log A/T)	Number of Event Detections: P-Wave Arrival Time
GBA	36.2	182	29	49
GDH	56.1	342	22	40
GRF	42.3	297	35	46
GRR	49.8	301	31	47
HAU	45.9	297	34	50
HFS	31.2	311	34	50
HOF	41.6	297	19	41
HYB	32.4	181	45	49
INK	59.7	13	28	38
ISK	35.4	275	0	43
JAS	90.9	15	1	52
KBS	37.1	343	2	42
KDC	64.7	28	0	44
KEV	31.3	328	47	52
KHC	41.2	295	41	52
KIC	81.1	269	0	46
KIR	33.5	324	12	47
KJF	30.3	317	44	51
KON	39.3	311	2	50
KRA	37.0	294	43	49
KYS	46.2	84	1	38
LBF	47.8	297	28	47
LFF	50.8	296	28	46
LJU	42.0	290	7	43
LMR	48.4	291	30	46
LOR	47.7	297	30	50
LPF	50.1	301	24	41
LPO	50.7	296	25	42

Table 2 (Cont'd)

Station Code	Δ°	AZ°	Number of Event Detections: m_b (or log A/T)	Number of Event Detections: P-Wave Arrival Time
LRG	48.4	292	34	47
LSF	49.6	297	29	44
MAT	44.2	84	30	47
MFF	50.4	299	27	45
MHC	91.0	16	0	47
MIN	88.3	16	0	47
MLR	35.3	284	0	40
MNT	82.0	341	24	39
MOX	41.3	293	48	52
MUN	88.0	149	13	38
NEW	81.3	11	15	49
NUR	31.8	310	48	52
OTT	82.6	342	33	40
PMG	83.6	113	23	39
PMR	62.4	24	42	46
PNT	79.9	12	33	40
POO	31.5	189	19	41
PRI	92.6	16	0	44
PRU	40.2	296	43	48
RJF	50.2	296	30	38
SES	79.7	6	26	40
SIT	69.7	19	0	42
SOD	31.0	324	0	52
SSC	49.3	301	29	45
SSF	48.1	297	31	49
STU	43.9	297	31	38
TCF	49.2	297	32	47
TOL	56.7	294	22	43

Table 2 (Cont'd)

Station Code	Δ°	AZ°	Number of Event Detections: m_b (or log A/T)	Number of Event Detections: P-Wave Arrival Time
TRO	34.2	327	1	44
TSK	45.6	83	8	38
TUL	94.4	356	42	44
UCC	45.6	301	4	49
UME	33.6	317	0	43
UPP	35.4	310	31	52
VKA	40.0	293	8	48
VRI	34.6	284	0	43
WIT	43.4	303	0	48
ZUL	45.0	295	0	42
WDC	88.0	16	0	47

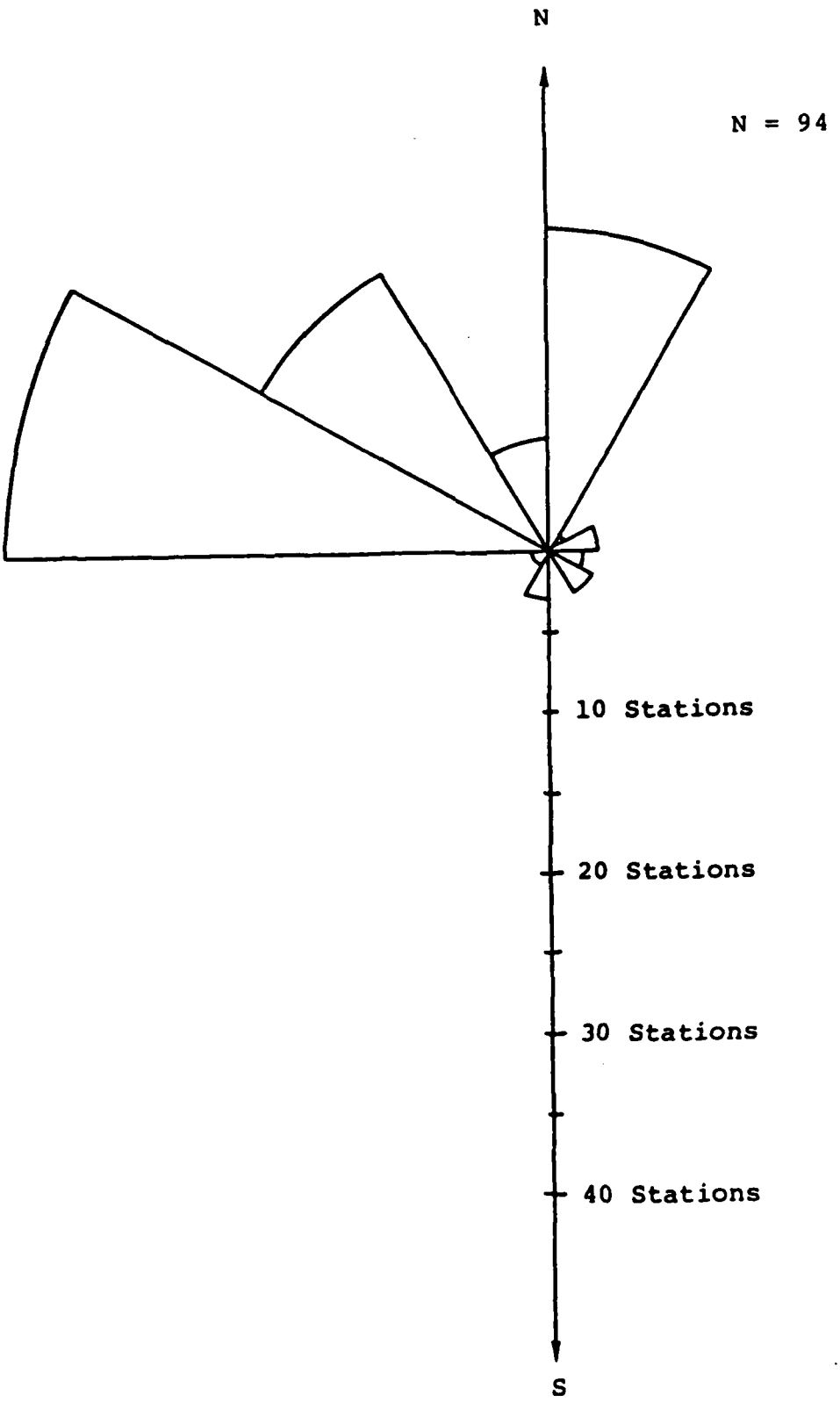

Figure 5. Azimuthal station coverage for the initial station network used in this study.

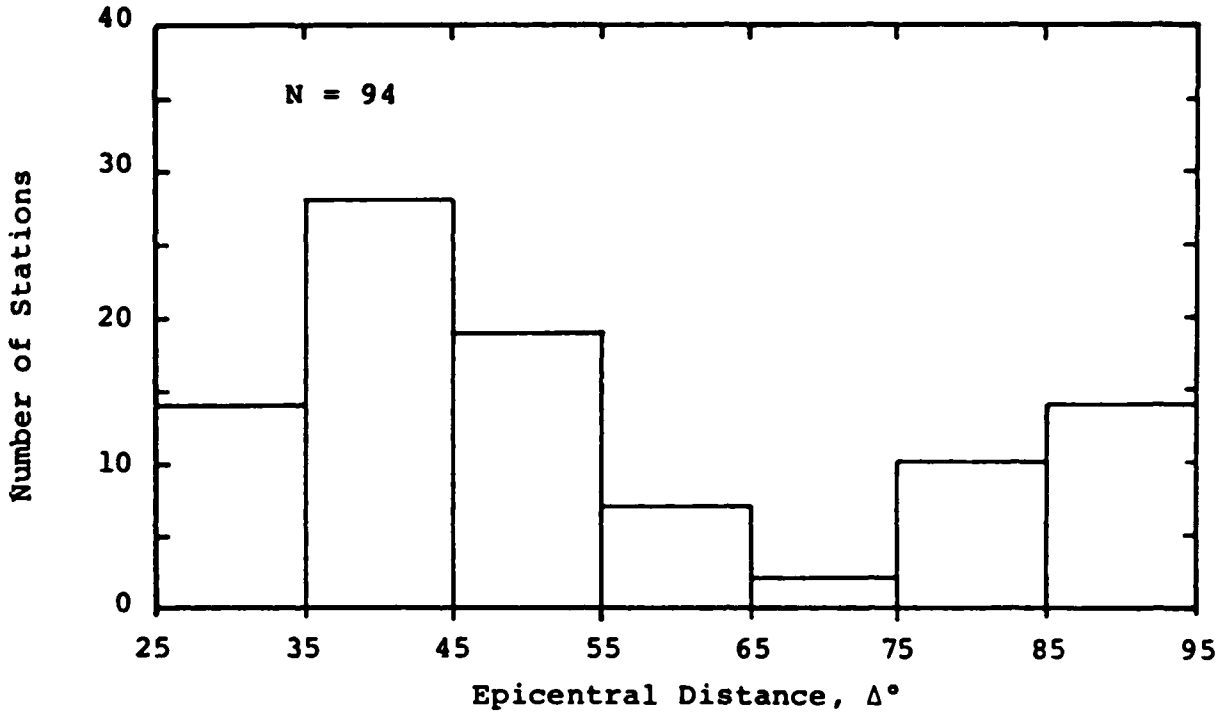

Figure 6. Histogram showing the frequency distribution of network stations by epicentral distance to the center of the Shagan test site.

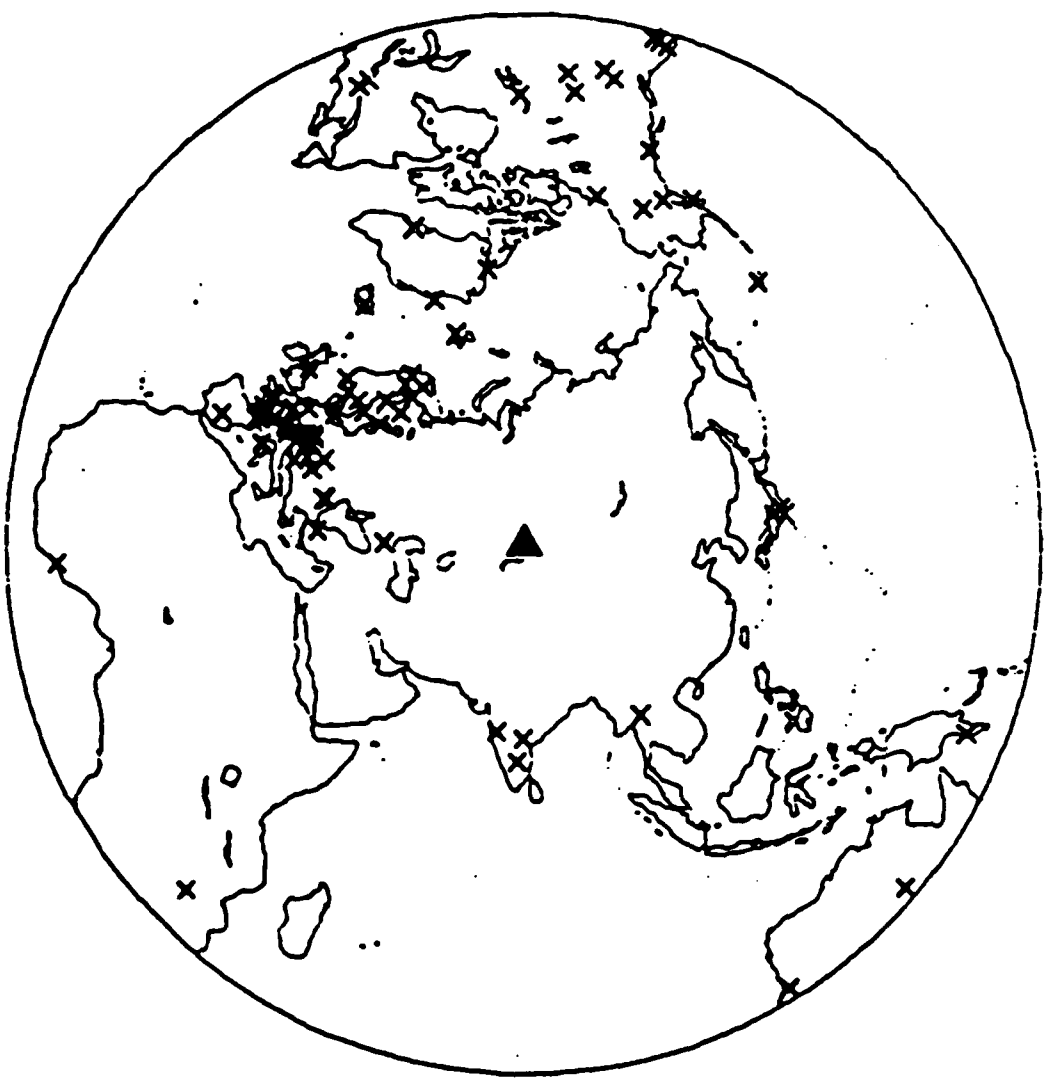

Figure 7. Map locations of stations shown on an azimuthally equidistant projection centered on the Shagan River test site, denoted by solid triangle (▲).

III. ANALYSIS OF THE TELESEISMIC P WAVE DATA

3.1 m_b DATA

The m_b data base which was described in detail in the preceding section has been subjected to a variety of statistical analyses in an attempt to identify any systematic geophysical variations within the Shagan River testing area. For the purposes of this investigation, the individual station m_b values have been initially processed using the LSMF (least squares matrix factorization) procedure originally described by Douglas (1966). Under this formulation, data recorded on a network of stations from explosions at a given test site are statistically analyzed to simultaneously determine the best-fit station correction factors and network-averaged magnitudes for each event, under the constraint that the station correction factors sum to zero. The principal advantage of this approach is that it provides a consistent framework for analyzing data recorded on networks of stations for which different stations have recorded different numbers of the events under consideration. In the context of the present study, it is important to note that the "station corrections" computed using the LSMF procedure actually represent the composite of effects at the source, along the propagation path and at the receiver which cause the m_b values at a particular station to be consistently different from the corresponding large network average m_b values. Thus, for explosions at a particular test site, the "station corrections" may be more closely associated with propagation effects near the source than with variations in the crustal structure beneath the receivers. A dramatic example of this fact is provided in Figure 8 which shows a comparison of network-averaged m_b values for selected explosions at the Degelen Mountain and Shagan River testing areas of the Semipalatinsk Test Site with the corresponding

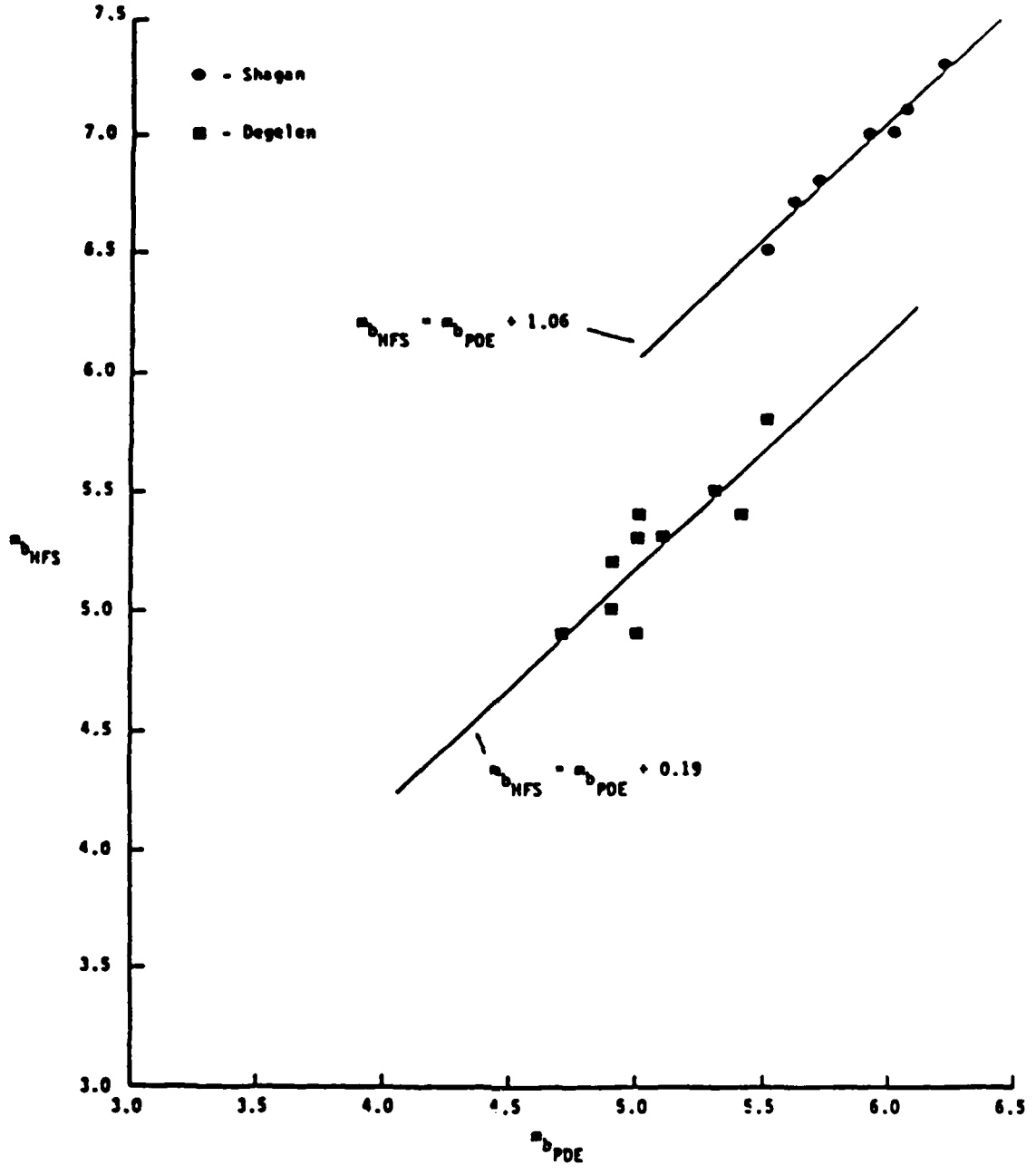

Figure 8. Comparison of single station HFS and PDE network m_b values for underground nuclear explosions at the Degelen and Shagan River test sites.

m_b values observed at station HFS (Hagfors) in Sweden. Note that the m_b data for the two areas segregate into two disjoint populations such that, for a fixed value of network m_b, the HFS m_b values are nearly a full order of magnitude larger for explosions at Shagan than for explosions at Degelen. That is, the HFS m_b "station correction" factor with respect to the worldwide average changes by nearly a full order of magnitude between these two test sites which are separated by less than 60 km, presumably reflecting near-source propagation path effects associated with the well-known differences in the near-surface geologic environments at the two sites (i.e., granitic intrusives at Degelen versus sedimentary formations at Shagan). This example demonstrates that teleseismic m_b variations do correlate with variations in test site conditions, at least in some cases.

The analysis of the Shagan River data set was initiated by running an LSMF analysis on the individual station m_b data recorded from the selected 52 explosions described in Section II. A total of 71 stations which reported m_b values for 5 or more of these explosions were included in this preliminary evaluation. This number was subsequently reduced to 59 by eliminating those stations for which the computed standard error of estimate in the mean station correction exceeded 0.3 magnitude units. This judgment was made on the basis of the observation that the average standard error of estimate in the mean station correction for the final 59 stations is less than 0.2 magnitude units. The number of events for which m_b values were reported, for each of these 59 stations, are displayed in histogram form in Figure 9 where it can be seen that all but 7 of these stations reported m_b values for at least 20 of the 52 selected Shagan River explosions. An LSMF analysis was run on this final data set to obtain the network-averaged m_b values and average station corrections to be used in the subsequent

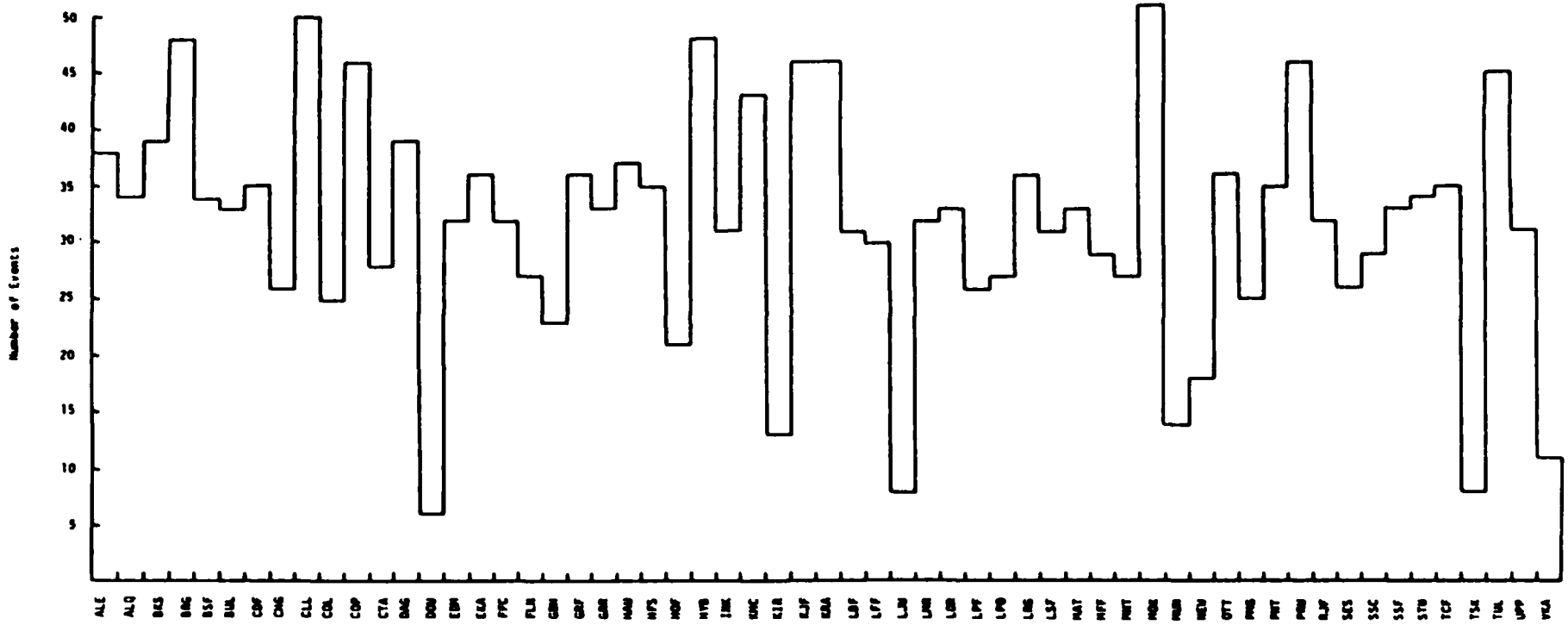

Figure 9. Histogram showing the number of events with m_b data recorded by each stable station in network after LSMF analysis.

investigations. The results of these calculations were found to be quite consistent with those reported by Marshall et al. (1984) on the basis of their analysis of data recorded from a similar set of Shagan River explosions on a large, worldwide network consisting of 174 stations, of which 54 are in common with the network used in the present study. This consistency is graphically illustrated in Figures 10 and 11 where the network-averaged m_b values and station corrections estimated in the present study are compared with those of Marshall et al. (1984). Complete lists of the final network m_b values and station corrections derived in this study are presented in Tables 3 and 4 respectively. For purposes of comparison, the corresponding network m_b estimates obtained by Marshall et al. (1984) and the ISC are also included in Table 3 for those explosions for which they are available.

Having obtained average m_b station corrections for explosions at the Shagan River site, it now remains to examine variability within the test site itself. We have attempted to accomplish this through systematic evaluation of the observed distributions of station-corrected m_b residuals (i.e., corrected single station m_b - event m_b) as a function of source location. Now, in the absence of any underlying deterministic mechanisms, it would be expected that the residuals for a given station would be randomly distributed with respect to event location. However, this is not found to be the case at Shagan River. For example, Figure 12 shows the station-corrected m_b residuals as a function of event location for stations MAT and EKA. Note that the residuals, which can be regarded as variations in the "station corrections" with source location, show pronounced trends in that residuals of the same size and sign tend to cluster into geographical groups. This suggests that there are some unaccounted for source region physical mechanisms which are affecting the radiation of P wave

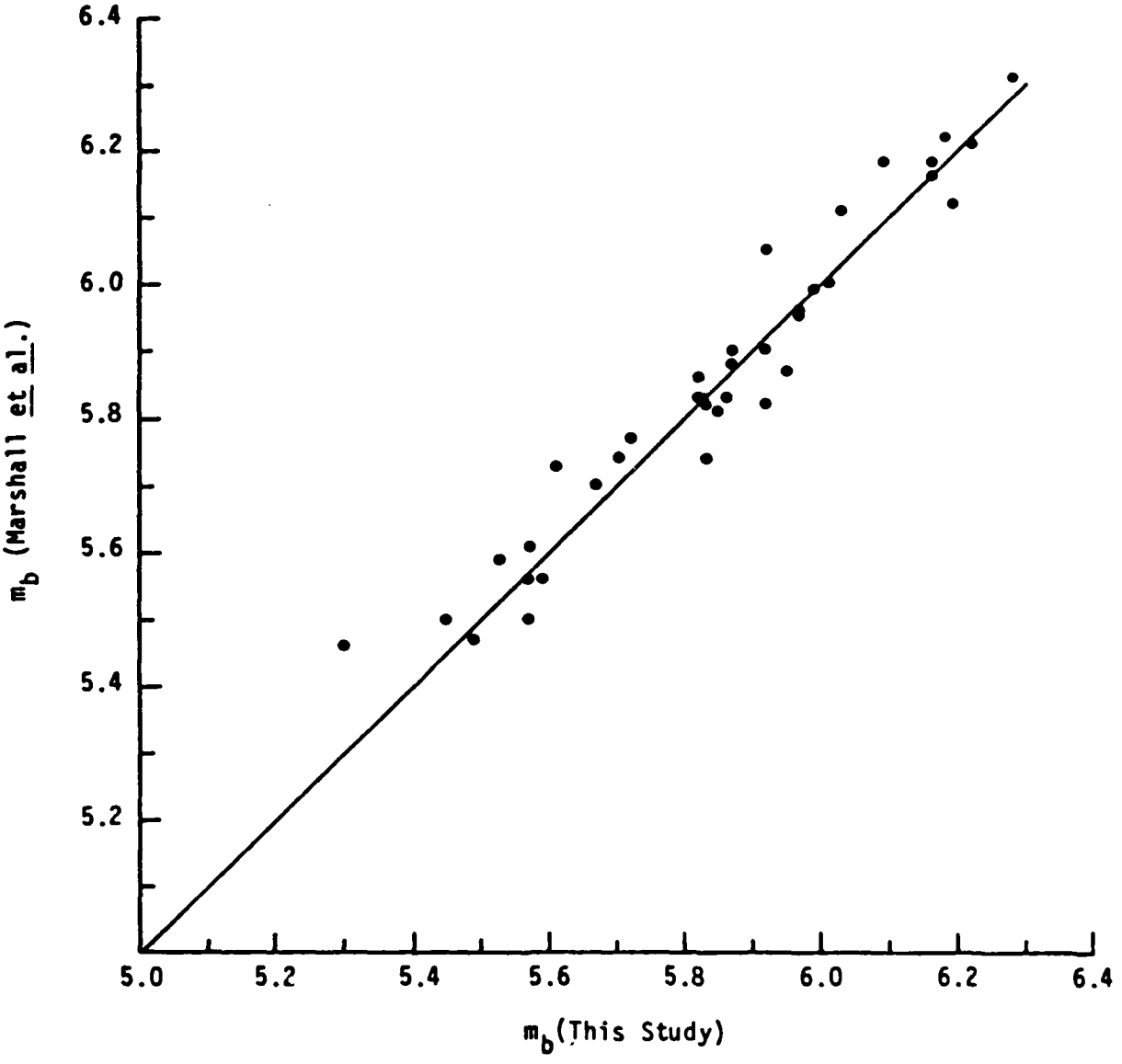

Figure 10. Comparison of network-averaged LSMF event magnitudes estimated in the present study with those of Marshall et al. (1984).

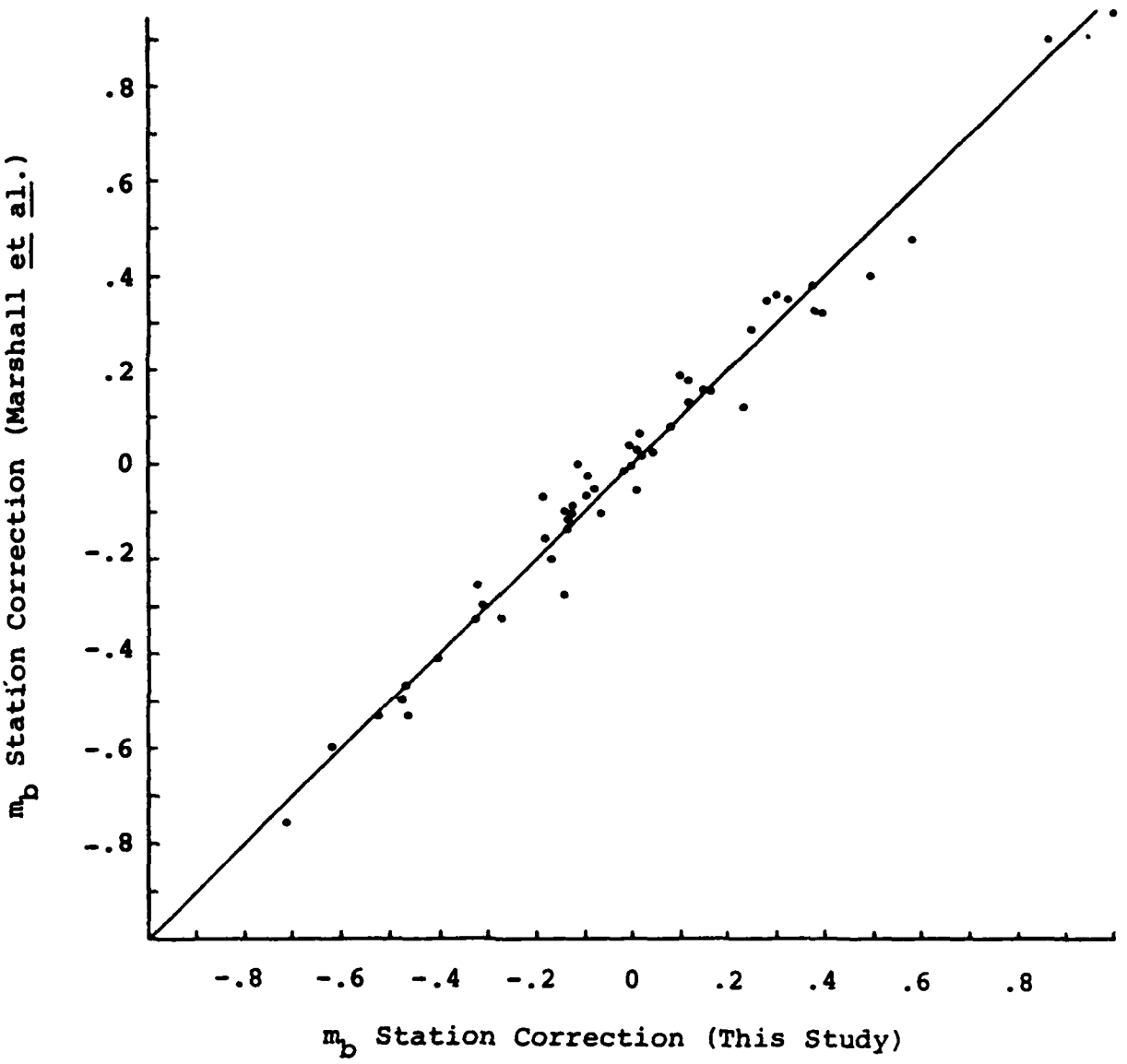

Figure 11. Comparison of m_b station corrections derived in this study with those of Marshall et al. (1984) for common stations.

Table 3

FINAL NETWORK m_b VALUES

Event No.	Date M D Y	This Study (# of Stations)	Marshall et al. (# of Stations)	ISC (# of Stations)
01	01/15/65	5.94 (7)	-	5.8 (11)
02	11/30/69	5.99 (24)	-	6.0 (65)
03	11/02/72	6.25 (11)	-	6.1 (75)
04	12/10/72	5.93 (3)	-	6.0 (26)
05	07/23/73	6.34 (12)	6.18 (60)	6.1 (81)
06	12/14/73	5.83 (24)	5.82 (54)	5.8 (67)
07	05/31/74	5.86 (25)	5.83 (70)	5.9 (83)
08	10/16/74	5.49 (18)	5.47 (57)	5.5 (63)
09	12/27/74	5.57 (20)	5.50 (50)	5.6 (60)
10	04/27/75	5.59 (25)	5.56 (60)	5.6 (71)
11	10/29/75	5.65 (13)	5.74 (55)	5.8 (64)
12	12/25/75	5.67 (20)	5.70 (59)	5.7 (70)
13	07/04/76	5.85 (26)	5.81 (66)	5.8 (83)
14	08/28/76	5.92 (41)	5.82 (73)	5.8 (82)
15	11/23/76	5.95 (42)	5.87 (76)	5.8 (93)
16	12/07/76	5.92 (31)	5.90 (60)	5.9 (76)
17	05/29/77	5.72 (32)	5.77 (77)	5.8 (97)
18	09/05/77	5.83 (22)	5.74 (84)	5.8 (97)

Table 3 (Cont'd)

Event No.	Date M D Y	This Study (# of Stations)	Marshall et al. (# of Stations)	ISC (# of Stations)
19	10/29/77	5.54 (24)	-	5.6 (53)
20	11/30/77	5.91 (30)	-	6.0 (90)
21	06/11/78	5.82 (38)	5.86 (76)	5.9 (92)
22	07/05/78	5.82 (35)	5.83 (81)	5.8 (96)
23	08/29/78	5.94 (35)	-	5.9 (80)
24	09/15/78	5.99 (37)	5.99 (80)	6.0 (100)
25	11/04/78	5.57 (46)	5.56 (95)	5.6 (106)
26	11/29/78	5.99 (35)	-	6.0 (82)
27	06/23/79	6.18 (46)	6.22 (103)	6.2 (121)
28	07/07/79	5.82 (40)	5.83 (90)	5.8 (109)
29	08/04/79	6.16 (49)	6.16 (110)	6.1 (137)
30	08/18/79	6.19 (50)	6.12 (115)	6.1 (135)
31	10/28/79	5.97 (46)	5.96 (103)	6.0 (127)
32	12/02/79	6.00 (37)	6.01 (98)	6.0 (118)
33	12/23/79	6.16 (44)	6.18 (94)	6.2 (116)
34	04/25/80	5.45 (43)	5.50 (89)	5.5 (103)
35	06/12/80	5.53 (41)	5.59 (74)	5.6 (91)
36	06/29/80	5.70 (39)	5.74 (69)	5.7 (88)
37	09/14/80	6.22 (32)	6.21 (83)	6.2 (104)
38	10/12/80	5.87 (41)	5.90 (91)	5.9 (118)

Table 3 (Cont'd)

Event No.	Date M D Y	This Study (# of Stations)	Marshall et al. (# of Stations)	ISC (# of Stations)
39	12/14/80	5.97 (40)	5.95 (94)	5.9 (115)
40	12/27/80	5.87 (28)	5.88 (72)	5.9 (90)
41	03/29/81	5.57 (40)	5.61 (83)	5.6 (105)
42	04/22/81	5.92 (49)	6.05 (96)	6.0 (127)
43	05/27/81	5.30 (39)	5.46 (75)	5.5 (93)
44	09/13/81	6.09 (51)	6.18 (100)	6.1 (131)
45	10/18/81	6.03 (30)	6.11 (77)	6.1 (111)
46	11/29/81	5.61 (41)	5.73 (82)	5.7 (109)
47	12/27/81	6.28 (45)	6.31 (91)	6.2 (128)
48	04/25/82	6.11 (32)	-	6.1 (121)
49	07/04/82	6.22 (43)	-	6.1 (114)
50	08/31/82	5.36 (38)	-	5.4 (78)*
51	12/05/82	6.18 (43)	-	6.1 (118)*
52	12/26/82	5.72 (46)	-	5.7 (98)*

* Magnitudes for explosions occurring after 08/31/82 are from the NEIS catalog.

Table 4

m_b STATION CORRECTIONS

Station	This Study (# of Events)	Marshall et al. (# of Events)
ALE	-0.404 (35)	-0.416 (32)
ALQ	-0.483 (31)	-
BKS	0.075 (36)	0.077 (33)
BRG	-0.458 (45)	-0.533 (40)
BSF	-0.179 (32)	-0.159 (29)
BUL	0.018 (32)	0.060 (44)
CDF	-0.618 (32)	-0.604 (31)
CHG	-0.111 (24)	-0.005 (20)
CLL	0.016 (48)	-0.061 (42)
COL	0.399 (25)	0.315 (22)
COP	-0.008 (44)	-0.019 (36)
CTA	-0.132 (25)	-0.141 (7)
DAG	-0.143 (37)	-0.280 (37)
DOU	0.372 (5)	-
EDM	0.377 (31)	0.371 (30)
EKA	0.170 (33)	0.153 (39)
FFC	0.325 (31)	0.347 (33)
FLN	0.289 (24)	0.343 (21)
GDH	0.016 (22)	0.031 (31)
GRF	-0.118 (35)	-0.112 (33)
GRR	-0.117 (31)	-0.097 (25)
HAU	0.003 (34)	0.037 (32)
HES	0.993 (34)	0.937 (43)
HOF	-0.057 (19)	-0.106 (14)
HYB	0.120 (45)	0.125 (37)
INK	0.501 (28)	0.393 (26)
KHC	-0.272 (41)	-0.329 (37)

Table 4 (Cont'd)

Station	This Study (# of Events)	Marshall et al. (# of Events)
KIR	0.970 (12)	-
KJF	0.582 (44)	0.471 (43)
KRA	0.242 (43)	0.122 (40)
LBF	-0.310 (28)	-0.293 (26)
LFF	-0.132 (28)	-0.101 (26)
LJU	-0.096 (7)	-
LMR	-0.182 (30)	-0.071 (27)
LOR	-0.096 (30)	-0.071 (34)
LPF	0.025 (24)	0.017 (20)
LPO	0.145 (25)	0.149 (21)
LRG	-0.087 (34)	-0.029 (30)
LSF	-0.466 (29)	-0.501 (26)
MAT	-0.711 (30)	-0.762 (16)
MFF	0.045 (27)	0.014 (24)
MNT	-0.132 (24)	-0.120 (18)
MOX	-0.072 (48)	-0.072 (41)
MUN	0.303 (13)	0.290 (11)
NEW	-0.459 (15)	-0.481 (14)
OTT	0.123 (33)	0.167 (30)
PMG	0.254 (23)	0.287 (22)
PNT	-0.172 (33)	-0.211 (32)
PRU	-0.513 (43)	-0.533 (40)
RJF	-0.317 (30)	-0.331 (27)
SES	0.391 (26)	0.312 (27)
SSC	0.097 (29)	0.183 (28)
SSF	-0.326 (31)	-0.274 (29)
STU	0.003 (31)	-0.062 (32)

Table 4 (Cont'd)

Station	This Study (# of Events)	Marshall et al. (# of Events)
TCF	-0.366 (32)	-0.339 (28)
TSK	-0.024 (8)	0.049 (8)
TUL	-0.043 (42)	-0.043 (41)
UPP	0.877 (31)	0.890 (28)
VKA	-0.129 (8)	-

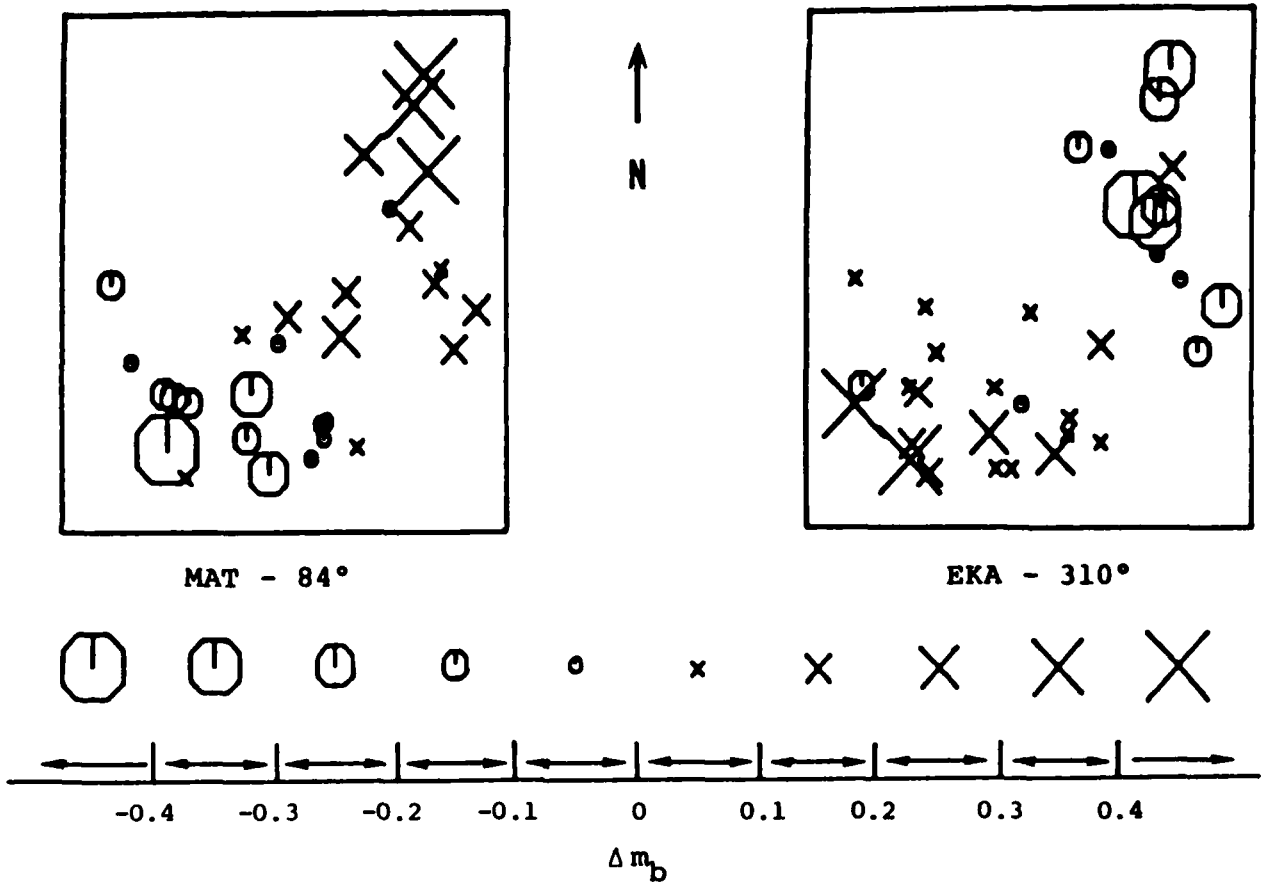

Figure 12. Station-corrected m_b residuals as a function of Shagan event location for stations MAT and EKA at the denoted recording azimuths.

energy to teleseismic distances. In an attempt to examine these effects in more detail, we have analyzed the azimuthal distribution of the corrected m_b residuals on an event-by-event basis. Figure 13 shows the results for four typical southwest Shagan events.* In these and subsequent polar coordinate plots (station azimuth measured clockwise from north), the circle corresponds to a corrected m_b residual of zero, while positive residuals plot outside the circle and negative residuals plot inside the circle according to the -0.5 to +0.5 m_b unit scale shown on the figure. Note from Figure 13 that for these explosions in the southwest portion of the test site, the corrected m_b residuals appear to be random at any given azimuth, and quite similar from event-to-event. However, as is illustrated in Figure 14, this simple picture does not hold for explosions in the northeast and central portions of the test site. It can be seen that in these areas there are some large variations (i.e., ± 0.5 m_b units) in the corrected m_b residuals with azimuth between events in very close proximity. On a more detailed level, it is difficult to quantitatively assess the magnitude of these variations from comparisons such as those shown in Figure 14 in that somewhat different networks of stations recorded each of these events. Therefore, in an attempt to eliminate any network biasing effects, we have also compared corrected m_b residuals for different pairs of events at common sets of stations. Four such comparisons are shown in Figures 15-18 for selected explosions located in the same area covered by Figure 14. It can be seen that these individual event comparisons at common stations are quite consistent with the general trends shown in Figure 14, confirming the fact that large variations in corrected m_b

* The event numbers (#) shown on this and subsequent figures are referenced to the event sequence numbers given in Table 3.

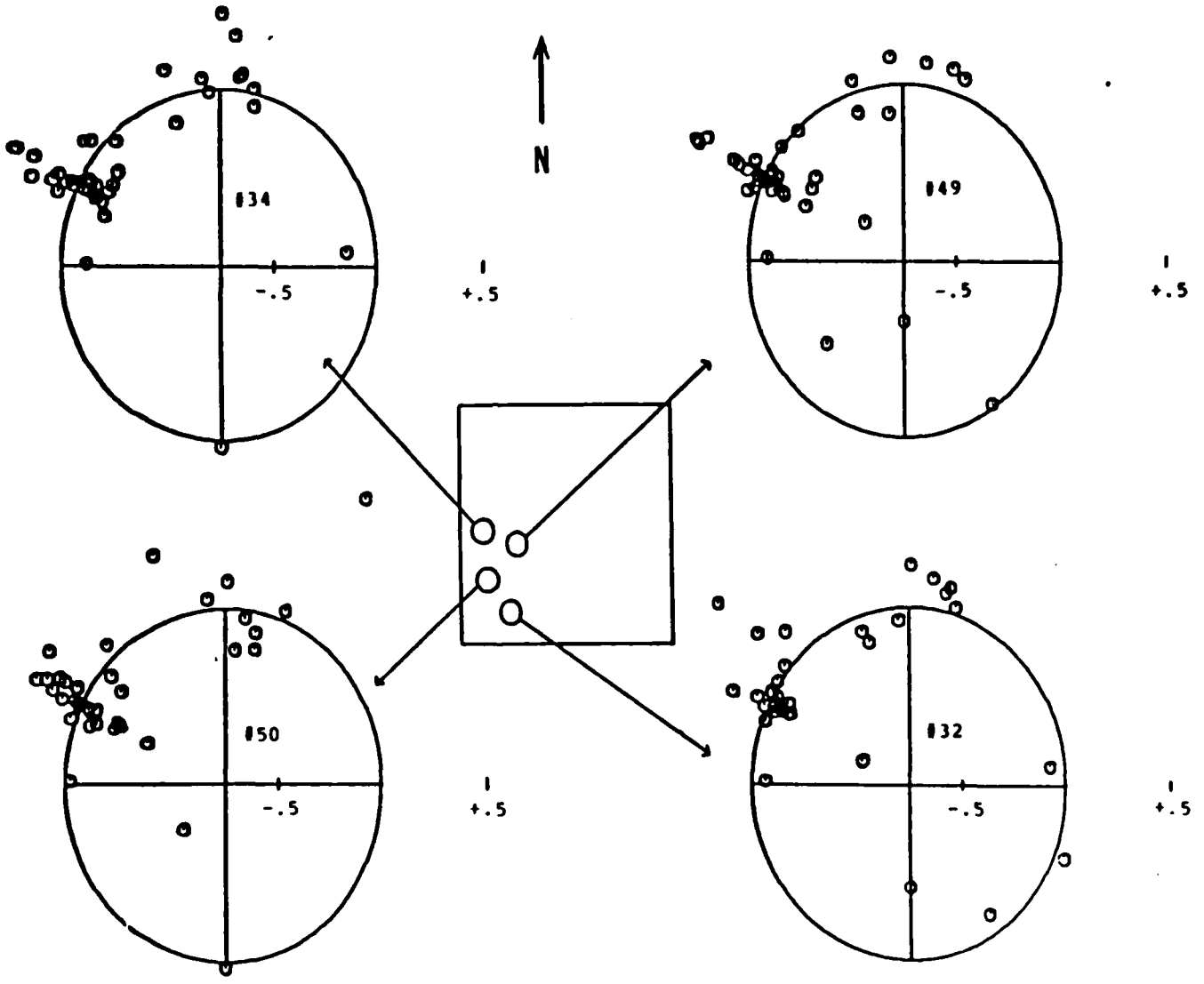

Figure 13. Azimuthal distribution of corrected m_b residuals as a function of event location; SW events. Circle represents zero residual; range -.5 m_b to +.5 m_b is denoted.

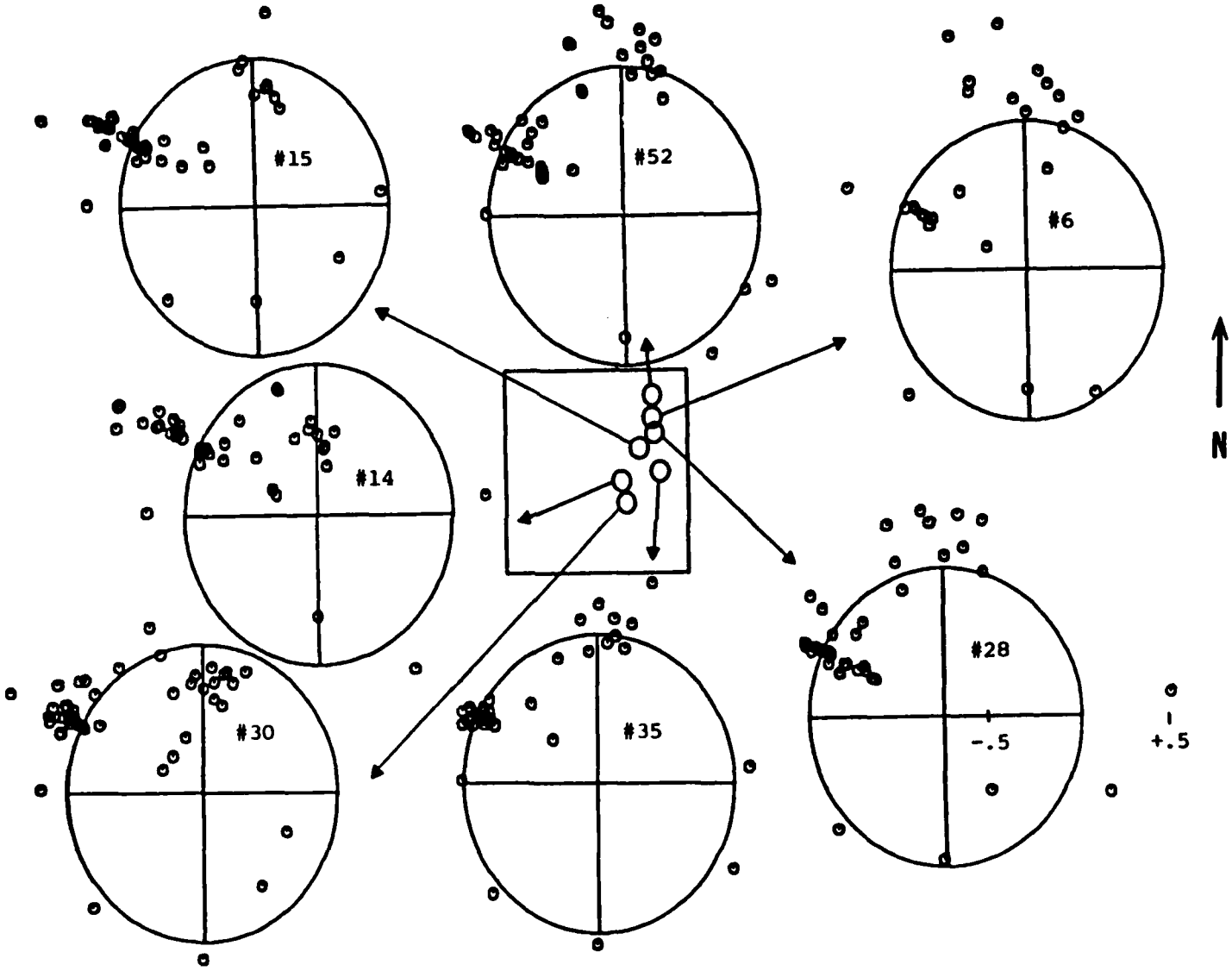

Figure 14. Azimuthal distribution of corrected m_b residuals as a function of event location; NE and central events. Circle represents zero residual; range -.5 m_b to +.5 m_b is denoted.

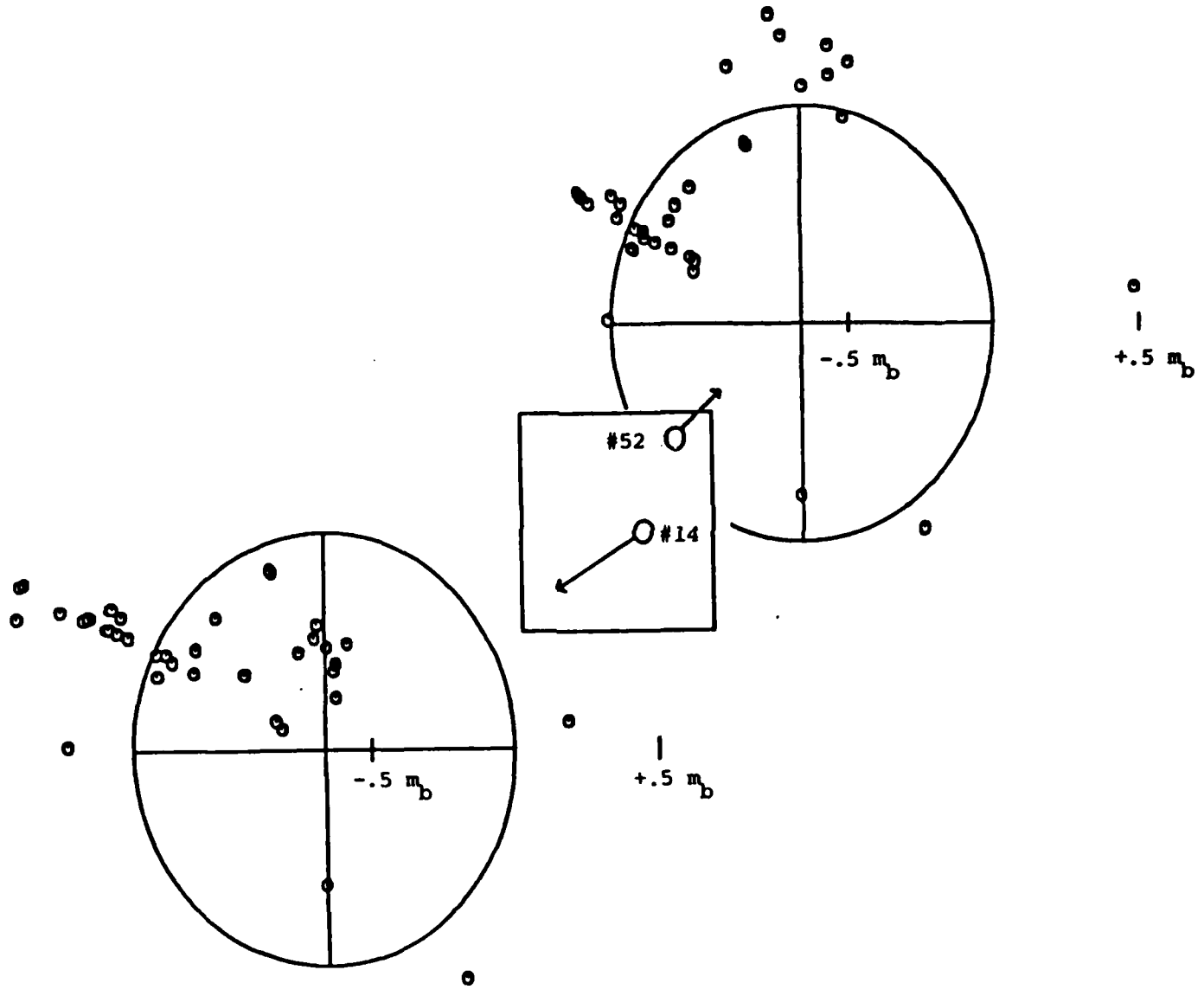

Figure 15. Comparison of corrected m_b residuals for events #52 and #14 at 34 common stations.

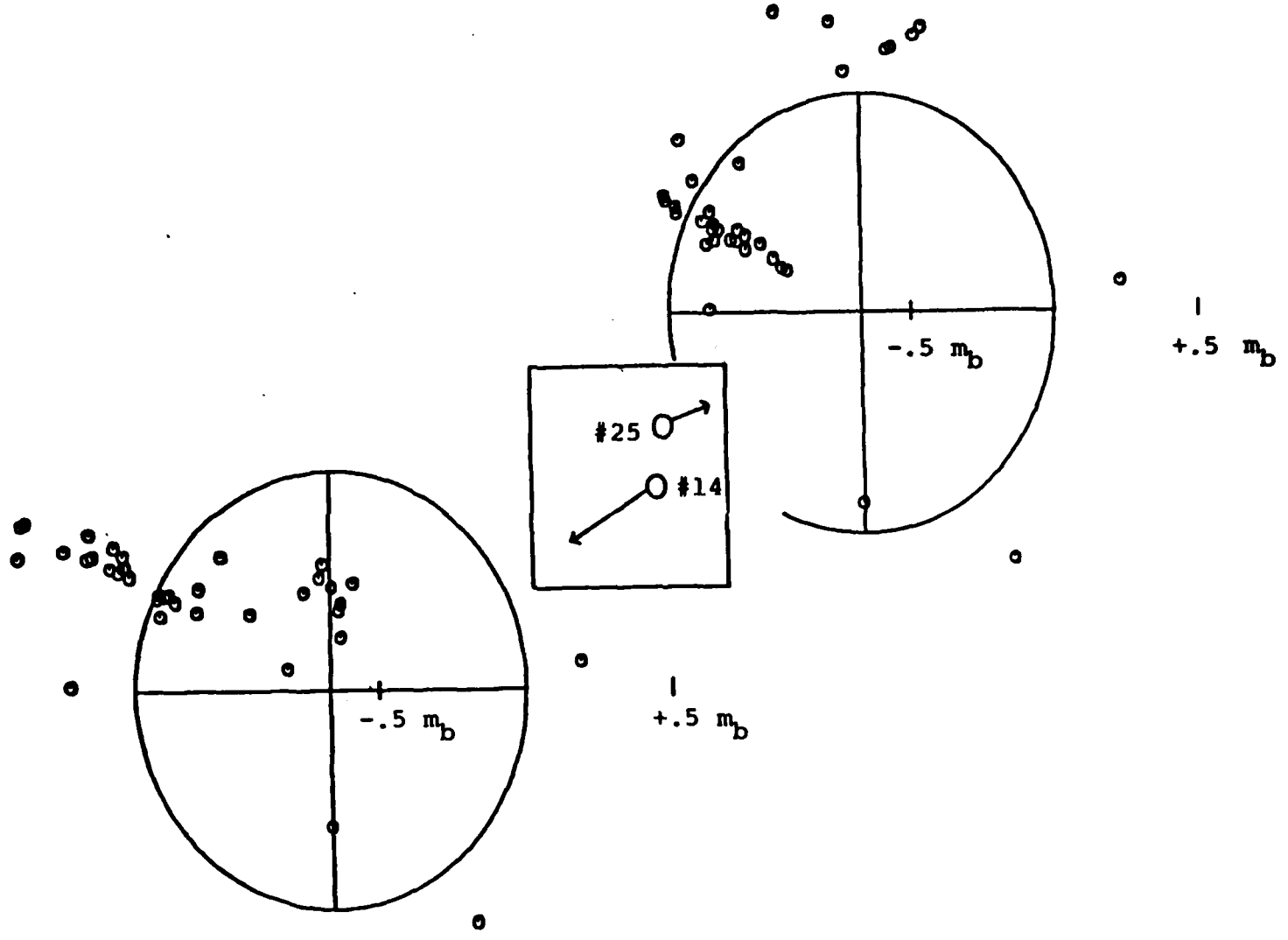

Figure 16. Comparison of corrected m_b residuals for events #25 and #14 at 37 common stations.

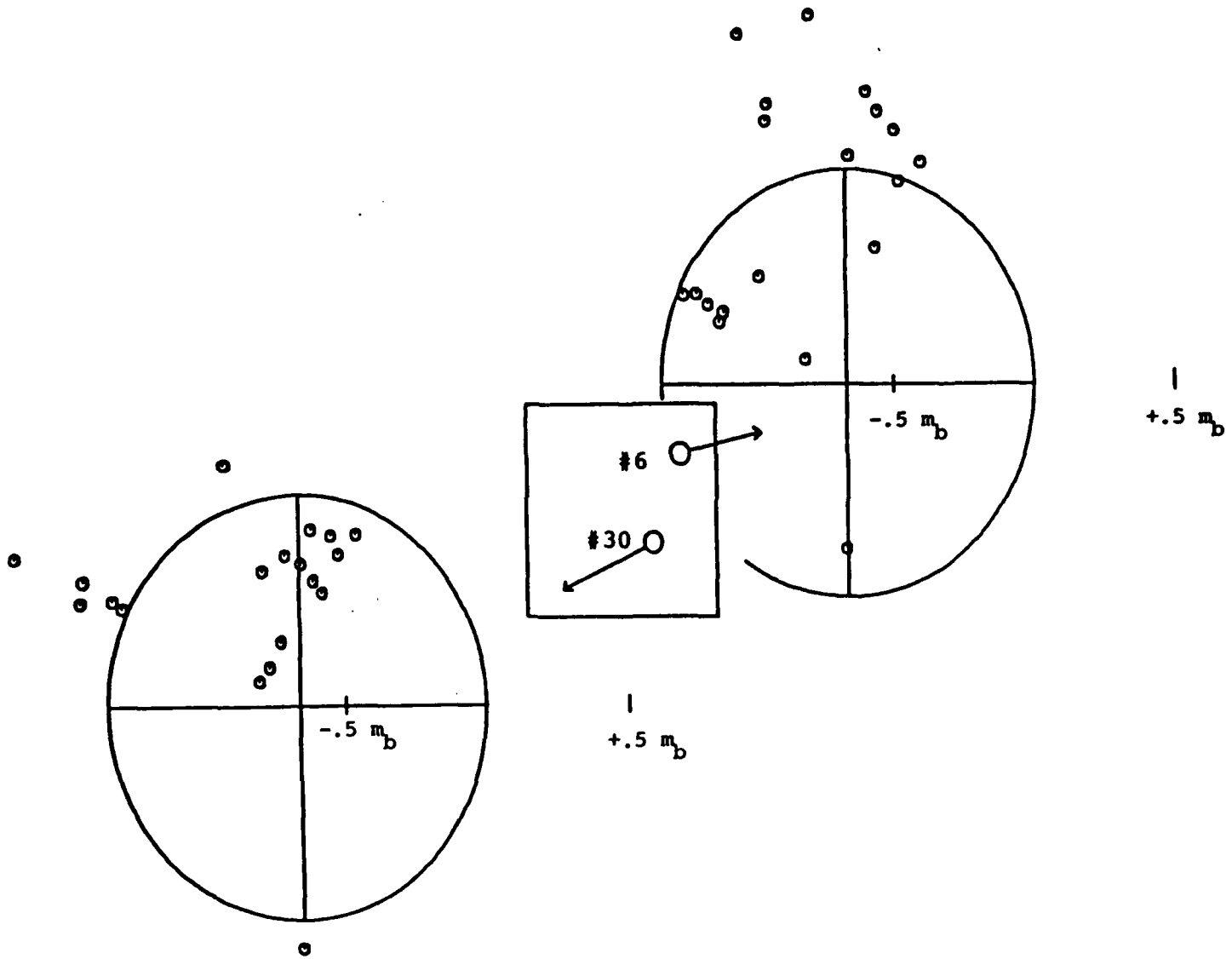

Figure 17. Comparison of corrected m_b residuals for events #6 and #30 at 22 common stations.

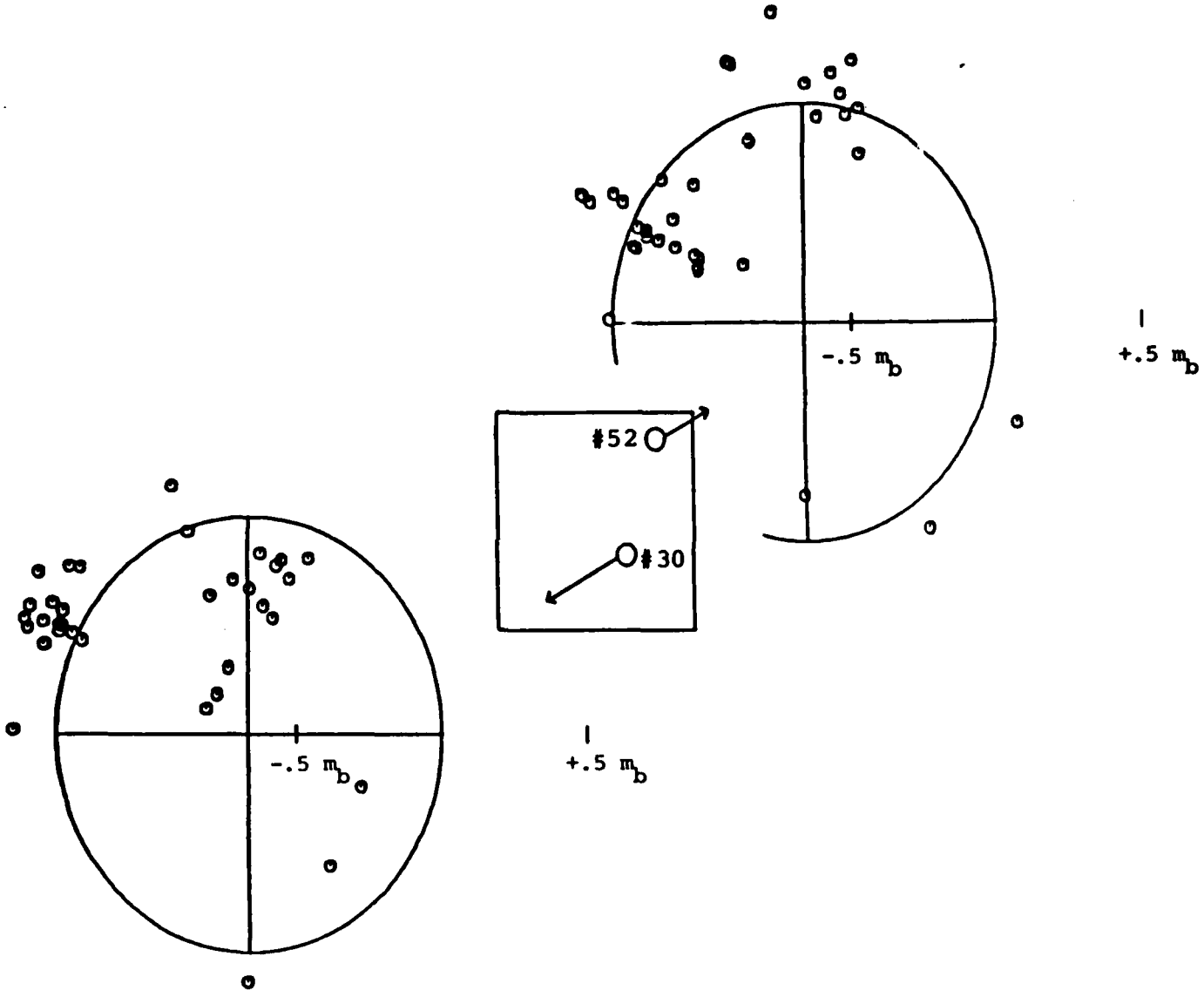

Figure 18. Comparison of corrected m_b residuals for events #52 and #30 at 43 common stations.

residuals do occur between events in close proximity in the northeast and central portions of the Shagan River test site. Specifically, explosions in the northeast quadrant (e.g., events #52, #25, and #6) show large positive corrected m_b residuals at stations in the northern azimuth window and predominantly negative corrected m_b residuals at stations in the northwest azimuth window, while explosions located nearer to the center of the test site (e.g., events #14 and #30) show opposite trends, with large negative corrected m_b residuals at stations in the northern azimuth and predominantly positive corrected m_b residuals at stations in the northwest azimuth. Moreover, these differences are large enough that they are statistically significant at a very high confidence level. This fact is illustrated in Figure 19 which shows the differences in the corrected m_b residuals at common stations between events #52 and #14 plotted as a function of azimuth. Note that the average m_b residual difference computed for stations in the 260° to 300° azimuth window is significantly different from that computed for stations in the 340° to 20° azimuth window, amounting to nearly 0.6 magnitude units. It follows that the network-averaged m_b values and corresponding yield estimates determined for these explosions will be highly dependent on the specific azimuthal distributions of the stations used to compute the averages. Thus, since yield estimation is generally accomplished using fixed networks of stations, some consideration must be given to the possible effects of network bias on the yield estimates for explosions in this portion of the Shagain River test site.

Given that the station-corrected teleseismic m_b data provide strong evidence of systematic geophysical variations within the Shagan River testing area, it now remains to attempt to identify specific causes of these variations. In the light of the evidence presented above, there are two alternate hypotheses which seem worthy of consideration:

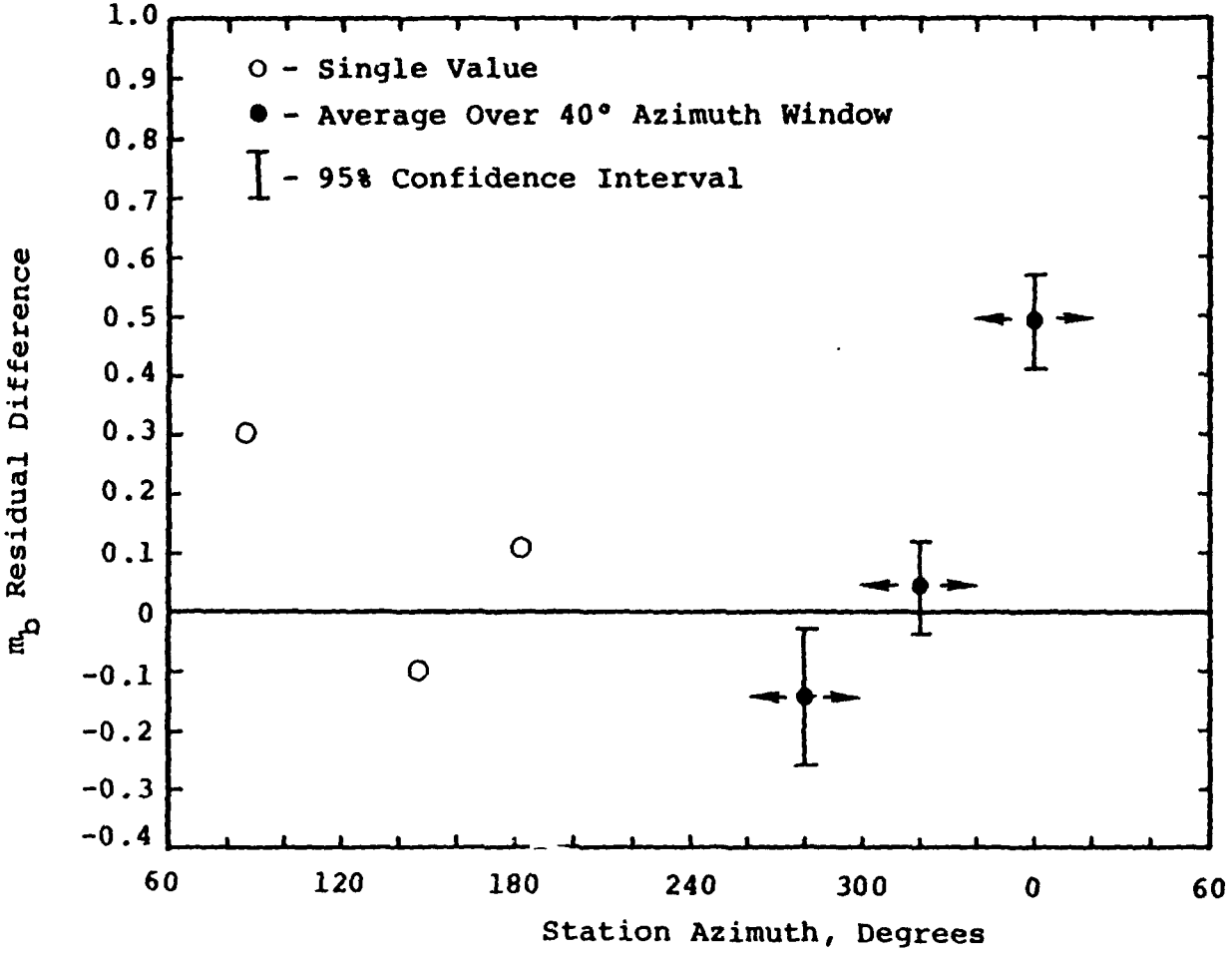

Figure 19. Station-corrected m_b residual differences between event #52 and event #14 as a function of station azimuth.

(1) that tectonic release induced by the explosions is affecting the short-period P waves and (2) that there are variations in the near-source P wave propagation paths to teleseismic distances as a function of source location within the test site. In principle, it should be fairly easy to discriminate between these two very different hypotheses. In fact, however, due to limitations in the distribution of teleseismic P wave observations with azimuth and epicentral distance, it is not easy to definitively test either hypothesis. For this reason, we have selected a control group of four nearby explosions in the northeast sector of the Shagan River testing area to be investigated in detail. The relative locations of these four explosions (e.g., #25, #28, #15 and #41, Cf. Table 3) within the Shagan River testing area are shown in Figure 20 where it can be seen that no two of the events are separated by more than 5 km. The letters A, B and C in parentheses beside the event numbers on this figure denote the tectonic release classification of these events assigned by North and Fitch (1981) on the basis of analyses of surface wave recordings from these events, where A denotes an explosion accompanied by a low level of long period Love wave excitation and no observed Rayleigh wave phase reversals, B denotes an explosion with observed Rayleigh wave phase reversals in some azimuths and C denotes an explosion with observed Rayleigh wave phase reversals at most stations. That is, in terms of the long-period surface waves an "A-type" explosion is interpreted to be one accompanied by a low level of tectonic release, while a "C-type" explosion shows convincing evidence of very strong tectonic release effects. Thus, as can be seen from Figure 20, the selected four events are not only closely spaced within the region where the azimuthal patterns of the corrected m_b residuals are changing rapidly, but also represent all three surface wave tectonic release classifications. It follows

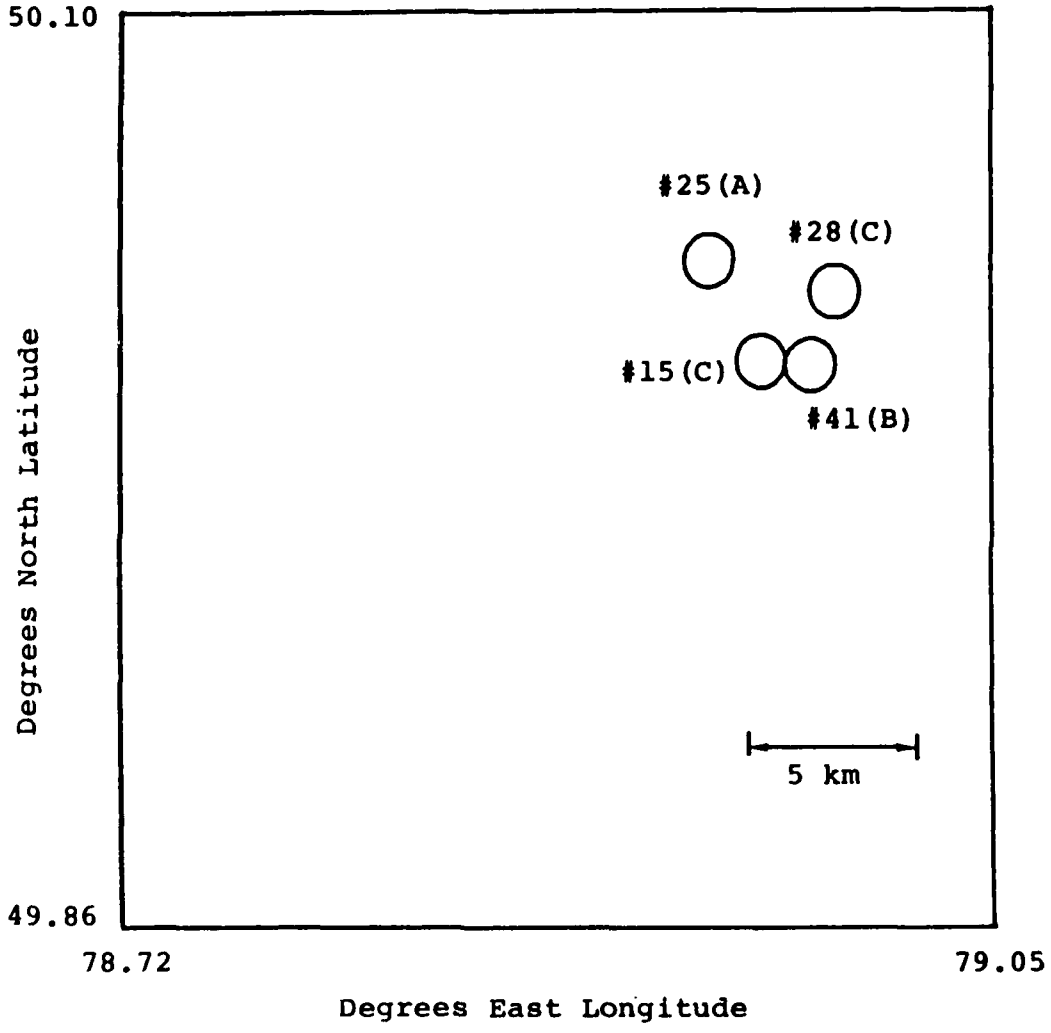

Figure 20. Map locations of Shagan River events #25, #28, #15 and #41 with respective tectonic release classifications from North and Fitch (1981).

that comparisons of data recorded from these explosions should provide some basis for evaluating the two hypotheses under consideration.

Regardless of which of the two hypotheses is correct, there should be some distance dependence to the corrected m_b residual pattern at a fixed azimuth associated with variations in P wave take-off angle at the source. Although the available data are not ideally distributed to define the details of such a distance dependence, they do seem to confirm its existence. For example, Figure 21 shows the corrected m_b residuals for the four events of Figure 20, plotted as a function of epicentral distance, Δ, using the data recorded at the 30 stations located in the narrow azimuth window $290° < \theta < 305°$. In both this and the next few figures, the stations are shown evenly spaced in order of increasing azimuth along the abscissa to permit the data from these tightly clustered stations to be differentiated from one another (i.e., the azimuth scale is nonlinear). The signs and sizes of the observed residuals are shown in terms of squares (positive) and triangles (negative) of varying sizes, keyed to the scale shown at the top of the figure. It can be seen from these four examples that there is indeed a pronounced distance dependence to the corrected m_b residuals at this northwest azimuth, characterized by a consistent change in sign of the residuals at an epicentral distance of about 45 degrees. Another noteworthy point is that the residual patterns seem to correlate better with event location than with tectonic classification. That is, the patterns for the two northern events (#25 and #28) shown at the top of Figure 21 are quite similar despite the difference in tectonic classification (i.e., A versus C) and different from those associated with the two southern events shown at the bottom of the figure which have been assigned tectonic classifications of B (#41) and C (#15).

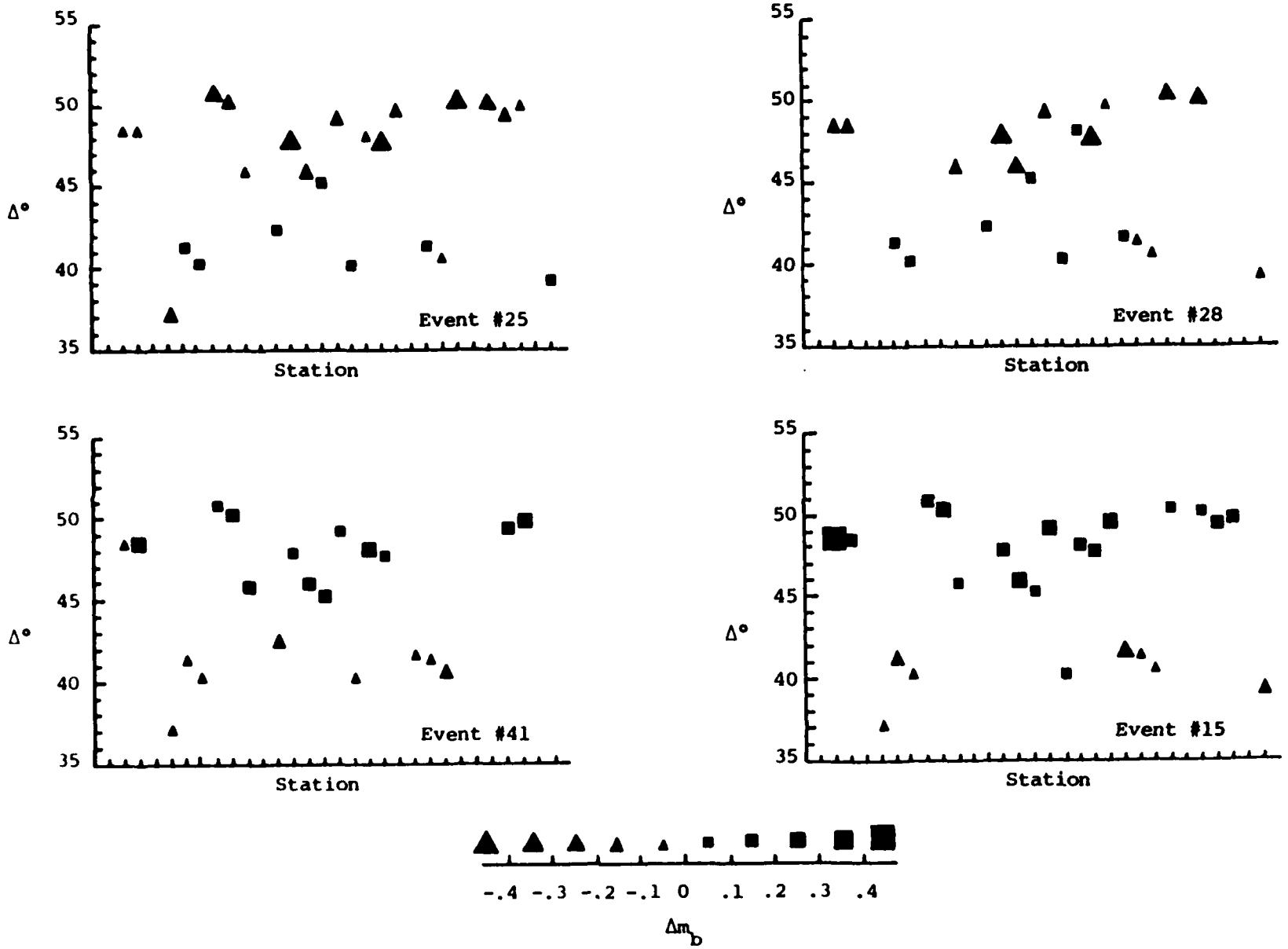

Figure 21. Corrected m_b residuals for events in Figure 20 as a function of epicentral distance determined for stations within the azimuthal range 290° < θ < 305°.

Specifically, the signs of the residuals at individual stations change in going from north to south, but not with tectonic classification. Moreover, it is also important to note that, for each of these four events, the average residual in the epicentral distance range of $45° < \Delta < 50°$ differs from that in the epicentral distance range $40° < \Delta < 45°$ by about 0.3 to 0.4 magnitude units, an amount which is significantly greater than the approximately 0.1 magnitude shift that would be theoretically predicted over this distance range for the generally inferred mode of tectonic release at Shagan (i.e., thrust motion on a fault plane dipping at about 45°). Although these results argue against a tectonic release explanation for the observed m_b variability, they are not really definitive in that they are representative of only a single narrow azimuth window. Unfortunately, the only other azimuth window for which there is enough data to make meaningful comparisons is the northern one which covers the range $340° < \theta < 20°$. The corrected m_b residuals for the four events of Figure 20 are plotted as a function of epicentral distance in Figure 22 using the data recorded at the 13 stations located in this northern azimuth window. It can be seen that at this azimuth data are available only over the epicentral distance range $45° < \Delta < 95°$ and that, over this range, there is no clear distance dependence to the corrected m_b residuals. However, as with the northwestern azimuth results shown in Figure 21, these residual patterns again appear to correlate better with event location than with tectonic classification, with the two northern events showing predominantly positive residuals and the two southern events showing predominantly negative residuals over this distance range.

Perhaps a more direct way of comparing the m_b data for the four events of Figure 20 is to compute the differences between the m_b residuals at common stations,

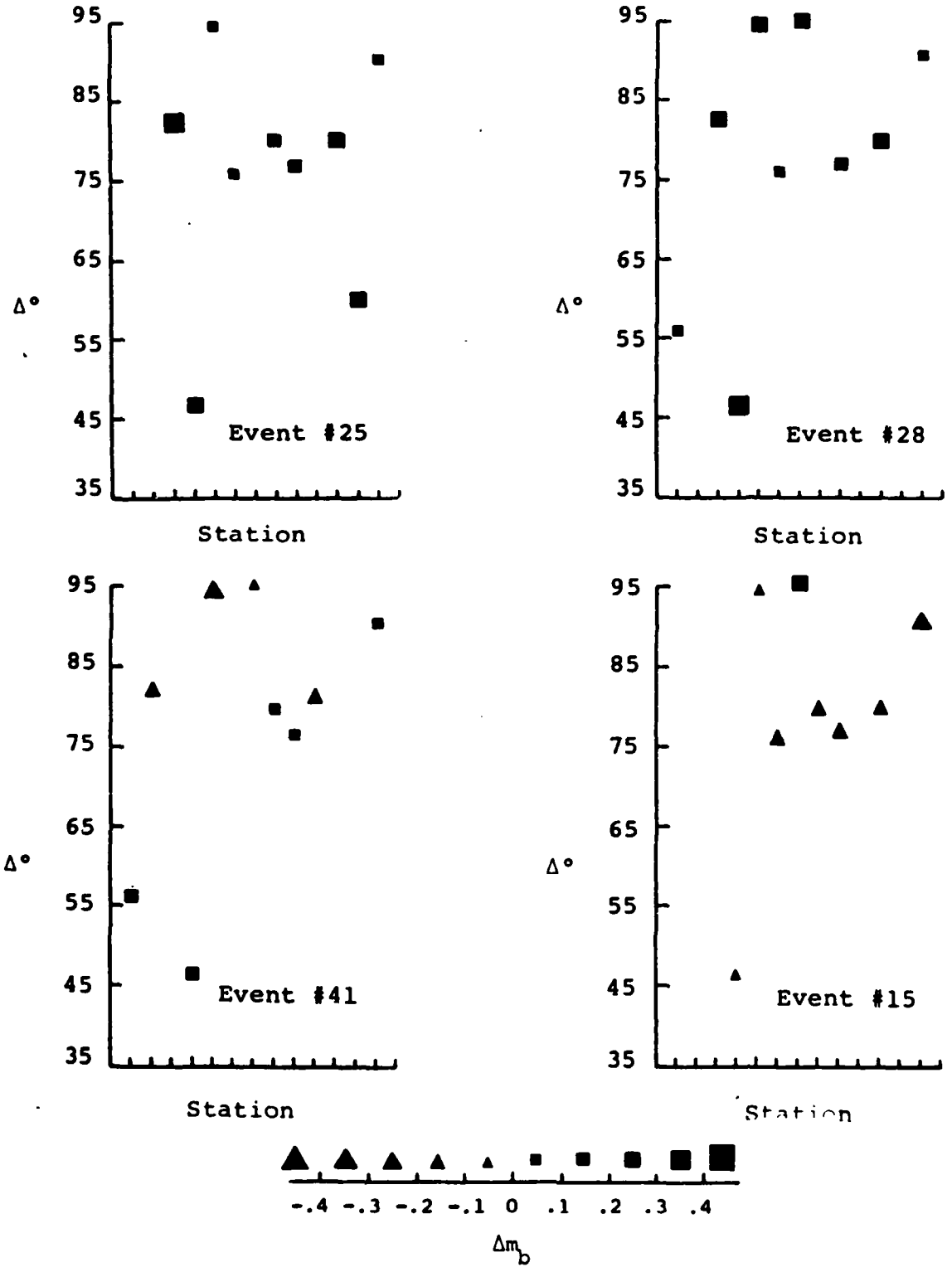

Figure 22. Corrected m_b residuals for events in Figure 20 as a function of epicentral distance determined for stations within the azimuthal range 340° < θ < 20°.

first for events with similar tectonic classification and then for events with similar locations. Figure 23 shows the differences in the m_b residuals at common stations plotted as a function of station azimuth for the two sets of events with similar tectonic classification (i.e., #15 versus #28 and #41 versus #25). Note that in both these cases there is evidence of pronounced azimuthal differences between the pairs of events with large positive residual differences to the northwest and large negative residual differences to the north. In contrast to this, Figure 24 shows the m_b residual differences at common stations computed for the pairs of northern (i.e., #28 versus #25) and southern (i.e., #41 versus #15) events. In this case, the residual differences shows no pronounced azimuthal dependence and are smaller, despite the fact that event #28 (C) is at a greater distance from event #25 (A) than from event #15 (C). These results strongly suggest that the variations in the azimuthal patterns shown in Figures 13-18 are related to event location rather than tectonic release effects and, thus, support the hypothesis that they are associated with variations in the near-source P wave propagation paths to teleseismic distances.

Considering the test site as a whole, if the observed azimuthal variations in the corrected m_b residuals with event location are indeed associated with variations in the subsurface geologic structure across the site, then it should be possible to contour the variations in station corrections as a function of source location. This in fact appears to be the case, although the limited spatial distribution and precision of the available explosion data makes it difficult to do anything more than outline the broad trends at the present time. For example, Figure 25 shows the average station-corrected m_b residuals as a function of event location, computed using the five stations in the

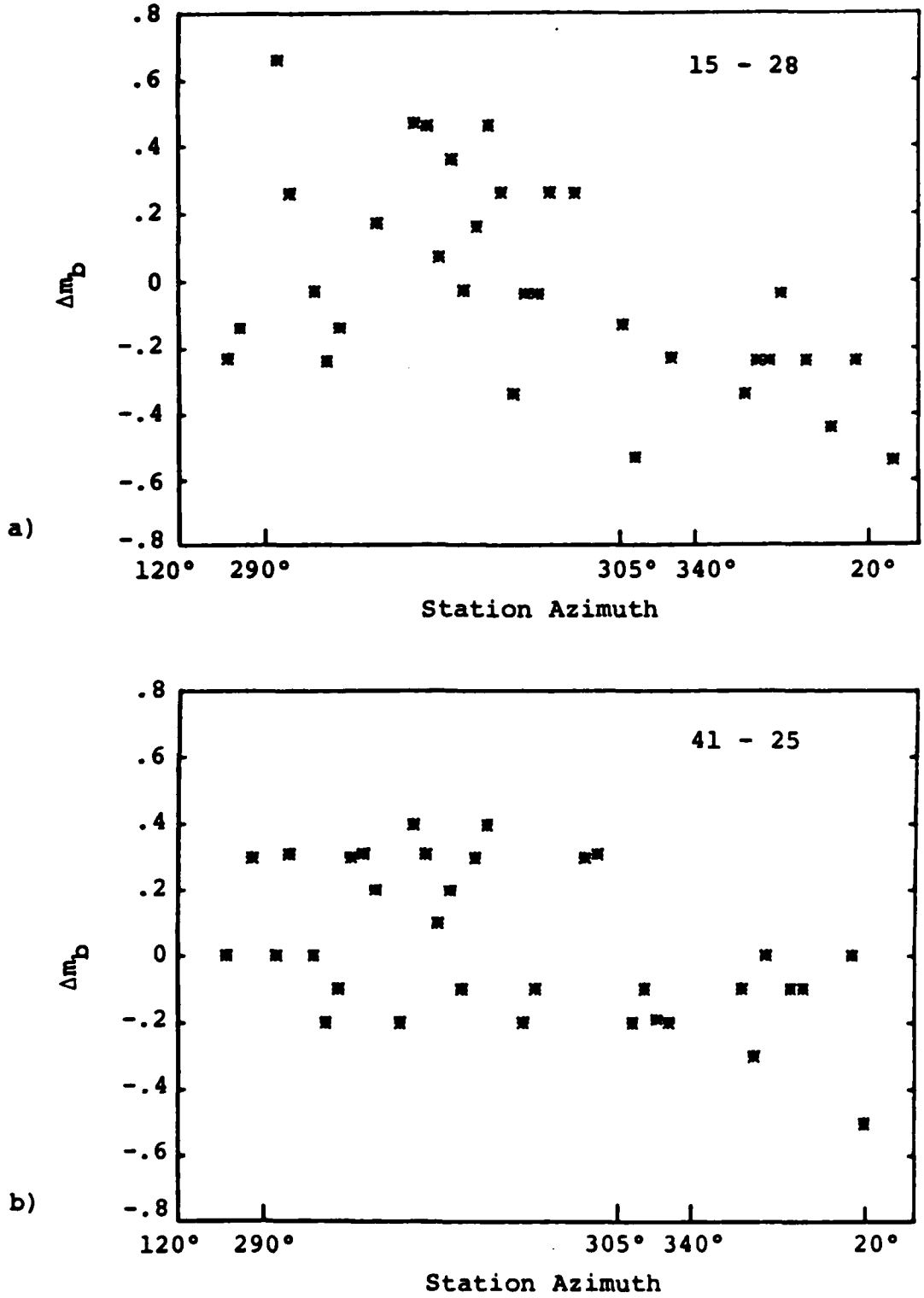

Figure 23. m_b residual differences, Δm_b, as a function of station azimuth for event pairs in Figure 20 with similar tectonic classifications: a) event #15(C) - event #28(C), and b) event #41(B) - event #25(A).

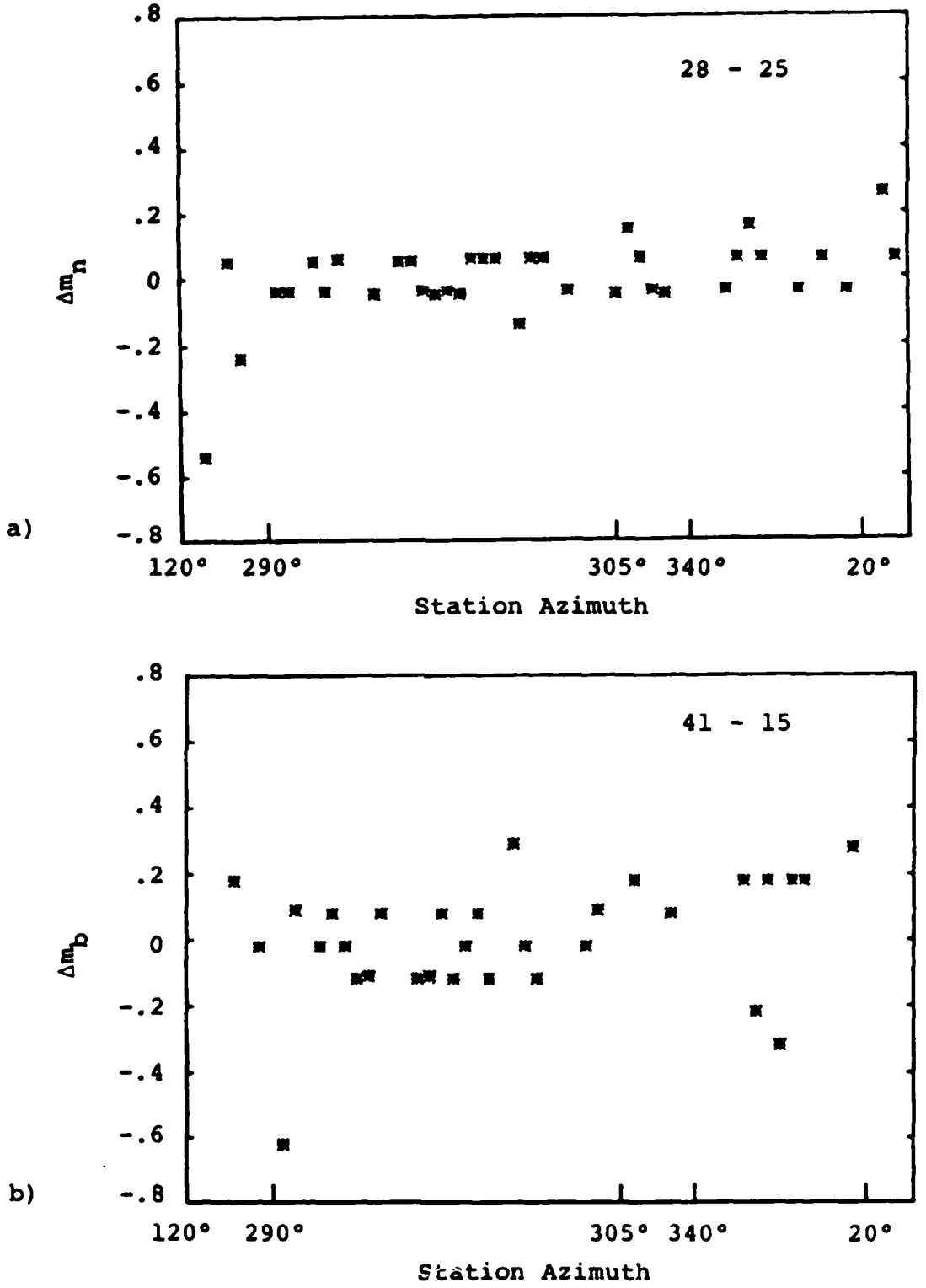

Figure 24. m_b residual differences, Δm_b, as a function of station azimuth for northern and southern event pairs from Figure 20. a) event #28(C) - event #25(A), and b) event #41(B) - event #15(C).

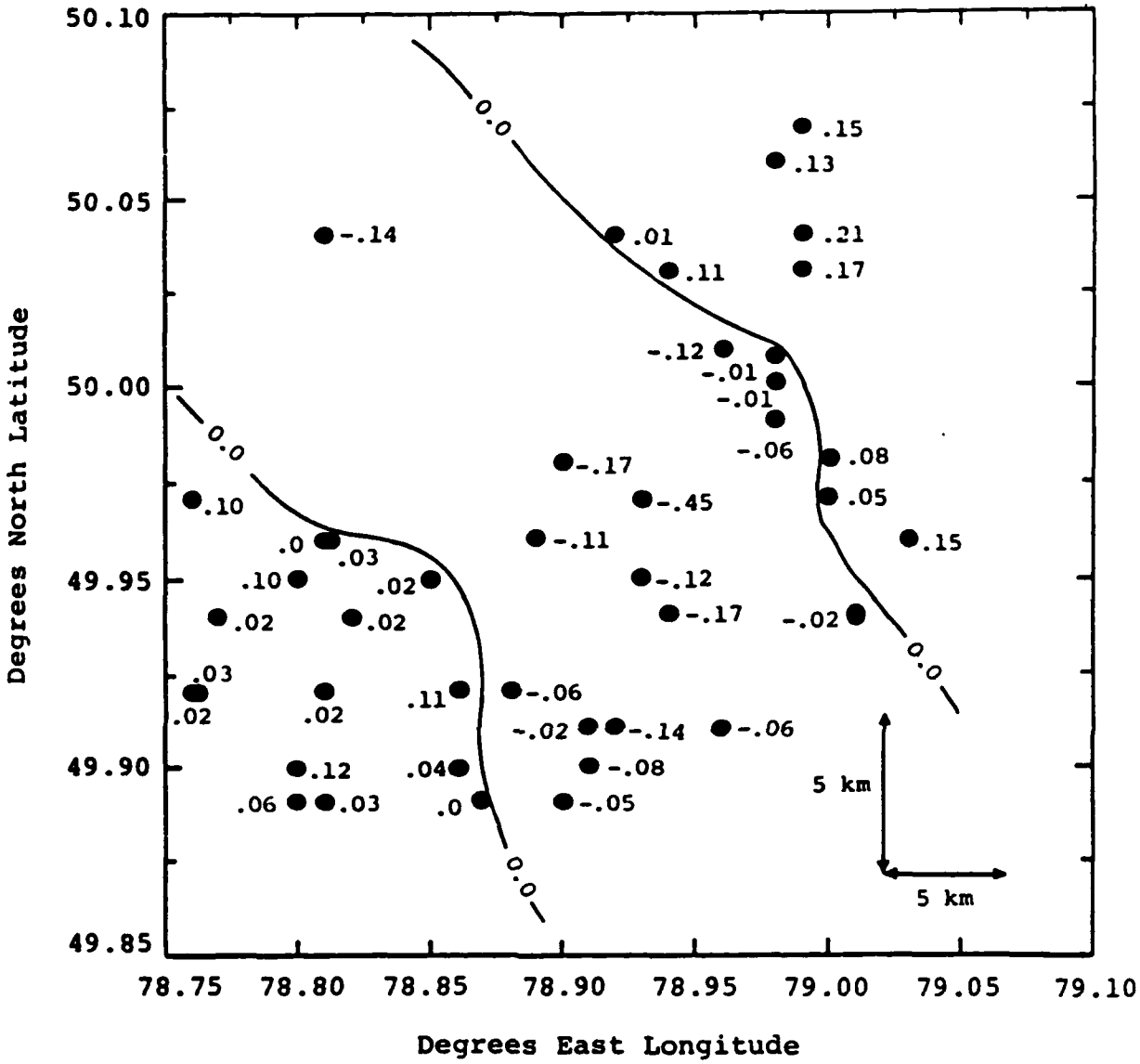

Figure 25. Contours of mean m_b residuals across the Shagan test site derived from a group of stations with an average recording azimuth of 3°. Contour is in m_b units. Solid circles are event locations.

northern azimuth (i.e., 340° < θ < 20°) which recorded 80 percent or more of the selected explosions. The computed 95 percent confidence intervals about the mean values shown on this figure average about ± 0.08 magnitude units, which provides some idea of the resolution of these data. Rough zero level contours have been drawn on this figure to highlight the general trends. It can be seen that, as was noted previously in conjunction with the discussion of Figure 13, the average station-corrected m_b residuals for events in the southwest portion of the test site are small and remarkably uniform over a broad area. In contrast to this, the average station-corrected m_b residuals for events in the northeast and central portions of the test site are relatively large and vary by more than 0.3 units m_b over distances of less than 5 km. However, despite the fact that this spatial variation is rapid, it is nevertheless a fairly systematic function of location, as can be seen with reference to the zero level contour drawn through that area. For purposes of completeness, the station-corrected m_b residuals for each of the 15 recording stations located in the northern azimuth window, including those used in deriving Figure 25, are shown as a function of event location in the central and northeast portions of the test site in Appendix A, where the zero level contour from Figure 25 has been superimposed on each station plot as a measure of the internal consistency of the complete data set.

The variation in the average station-corrected m_b residuals as a function of event location computed using the eight stations in the northwest azimuth (i.e., 290° < θ < 305°) which recorded 80 percent or more of the selected explosions is shown in Figure 26. In this case, due to the larger sample size, the computed 95 percent confidence intervals associated with the mean values shown on the figure average about ± 0.06 magnitude units. It can be seen from

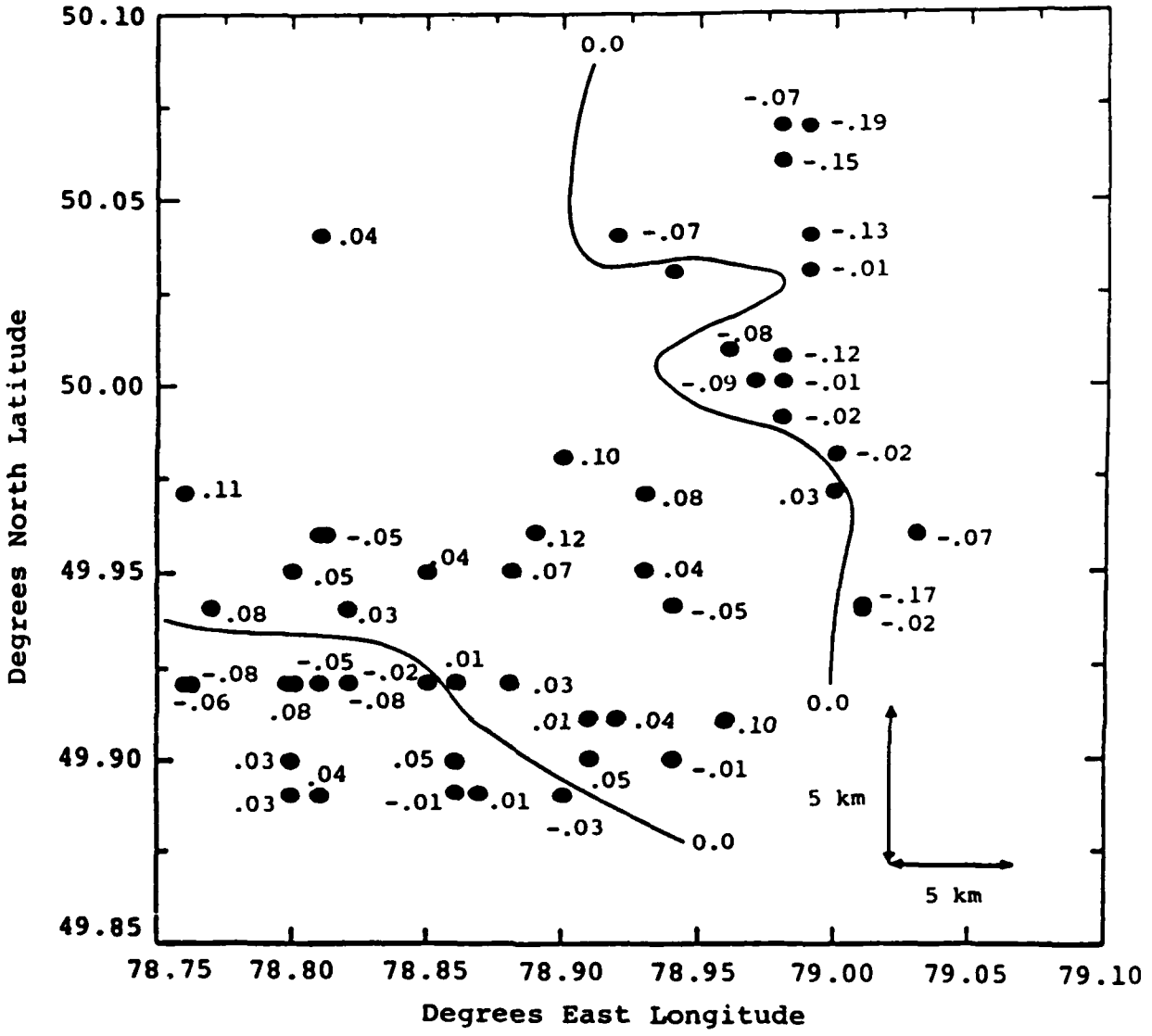

Figure 26. Contours of mean m_b residuals across the Shagan test site derived from a group of stations with an average recording azimuth of 300°. Contour interval is in m_b units. Solid circles are event locations.

this figure that the variations with event location for stations in the northwest azimuth are again fairly regular and similar, although opposite in sign, to those shown in Figure 25. The major difference between the two seems to be in the amplitude of the variation, which appears to be significantly greater for stations in the northern azimuth (Figure 25) than for stations in the northwest azimuth (Figure 26). However, this is deceptive in that the network-averaged m_b values used to compute the single station m_b residuals are heavily weighted by stations in the northwest sector, where more than half of the total number of stations are located. Thus, to some extent, the network-averaged m_b values are correlated with changes in P wave radiation to that azimuth and this tends to produce low apparent variability for stations in that azimuth. This can be understood more easily by reference to the following simple example. Consider the hypothetical case of an explosion with a true body wave magnitude m_{b_1} recorded by a network consisting of N_1 stations in the northwest (NW) azimuth and N_2 stations in the northern (N) azimuth. Then, the apparent magnitude of the event, $\tilde{m}_{b_1}$, will be given by

$$\tilde{m}_{b_1} = \frac{N_1 m_{b_1}^{NW} + N_2 m_{b_1}^{N}}{N_1 + N_2}$$

Suppose further that the northern observations are unbiased but that the northwest observations are biased. Specifically, let $m_{b_1}^{NW} = m_{b_1} - \Delta m$, $m_{b_1}^{N} = m_{b_1}$. It then follows that

$$\tilde{m}_{b_1} = m_{b_1} - \frac{N_1}{N_1 + N_2} \Delta m$$

Thus, for this event, the apparent m_b residuals for stations in the northwest (r_1^{NW}) and northern (r_1^{N}) azimuths will be given by

$$r_1^{NW} = m_{b_1}^{NW} - \tilde{m}_{b_1} = - \frac{N_2}{N_1 + N_2} \Delta m$$

$$r_1^{N} = m_{b_1}^{N} - \tilde{m}_{b_1} = \frac{N_1}{N_1 + N_2} \Delta m$$

It follows that, for example if $N_1 = 3N_2$, then

$$r_1^{NW} = - \frac{1}{4} \Delta m$$

$$r_1^{N} = \frac{3}{4} \Delta m$$

which illustrates how the actual bias in the northwest azimuth can be partitioned to give a large apparent bias in the northern azimuth. By the same line of reasoning, suppose for a second event that $m_{b_2}^{NW} = m_{b_2} + \Delta m$, where again $m_{b_2}^{N} = m_{b_2}$ and $N_1 = 3N_2$. In this case

$$r_2^{NW} = \frac{1}{4} \Delta m$$

$$r_1^{N} = - \frac{3}{4} \Delta m$$

and it follows that

$$r_1^{NW} - r_2^{NW} = - \frac{1}{2} \Delta m$$

$$r_1^{N} - r_2^{N} = \frac{3}{2} \Delta m$$

while

$$\left(r_1^N - r_2^N\right) - \left(r_1^{NW} - r_2^{NW}\right) = 2\Delta m$$

as it should. Thus, with reference to Figure 13, it is the difference between the average residual change in various azimuth windows that is well constrained, and not the absolute value of the residual change in any one azimuth. That is, the absolute Δm_b scale on that figure can be shifted up or down by changing the azimuthal distribution of the stations in the network. It follows that one cannot conclude from a comparison of Figures 25 and 26 that the variability is strongest at stations in the northern azimuth. What these figures do demonstrate is that the variability with source location is quite regular and most pronounced between the northeast and central portions of the test site, indicating that a change in the subsurface geology must occur in this vicinity.

3.2 P WAVE TRAVEL-TIME DATA

Analyses of travel-time data recorded from explosions at the Shagan River test site provide another potential means for investigating test site variability. In constrast to the m_b data discussed above, most of the stations report arrival time data for all the selected explosions which occurred during the period in which they were operational. In fact, on the average, 80 of the 94 stations discussed in Section II report arrival times for any given explosion. Our analysis of these data was initiated by transforming the reported arrival times into estimates of the travel times by subtracting the JED event origin times obtained by Marshall et al. (1984). Event-station distances were then computed using the JED explosion epicenters listed in Table 1 and

travel-time residuals were computed by subtracting the travel times predicted by the Herrin 1968 P wave travel-time curves (Herrin et al., 1968) from the observed travel times. Then, by analogy with the m_b analysis described above, the mean travel-time residual was determined for each station, and subtracted from the individual observed residuals at that station to obtain the variation of the residuals as a function of source location.

Unlike the m_b residual data, the reduced travel-time residuals were found to be quite small and to show no obvious correlation with event location. This is illustrated in Figure 27 which shows the reduced travel-time residuals as a function of event location at ten different stations representing a wide range of azimuths. It can be seen that these station-corrected travel-time residuals generally fall in the range of ± 0.5 seconds and appear to vary randomly across the test site. Similarly, Figure 28 shows the azimuthal distribution of the station-corrected travel-time residuals for the same central and northeast Shagan explosions for which m_b data were shown in Figure 14. As in the m_b plot, station azimuth in Figure 28 is measured clockwise from north, and the circle corresponds to a corrected travel-time residual of zero, with positive residuals plotting outside the circle and negative residuals plotting inside the circle according to the time scale shown on the figure. Comparing Figures 28 and 14, it can be seen that the corrected travel-time residuals do not show the systematic pattern of the corresponding corrected m_b residuals and appear to be randomly distributed about a mean of zero at all azimuths, independent of source location.

Thus, the observed travel-time residuals do not show any clear correlation with the corresponding m_b residuals. This is not a surprising observation and has, in fact, been frequently noted by previous investigators. Thus, for

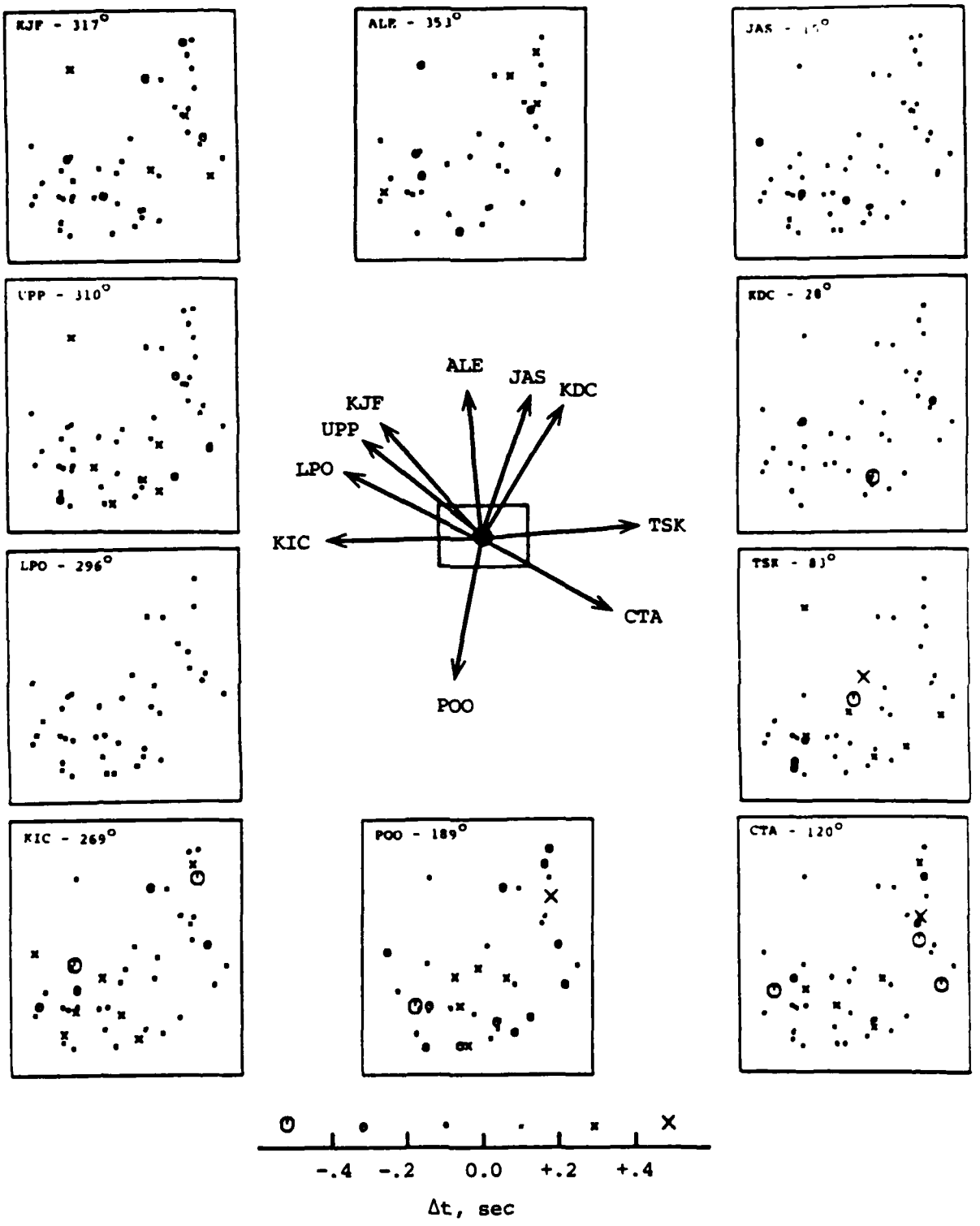

Figure 27. Reduced travel-time residuals, Δt, as a function of event location observed at several recording azimuths surrounding the Shagan test site.

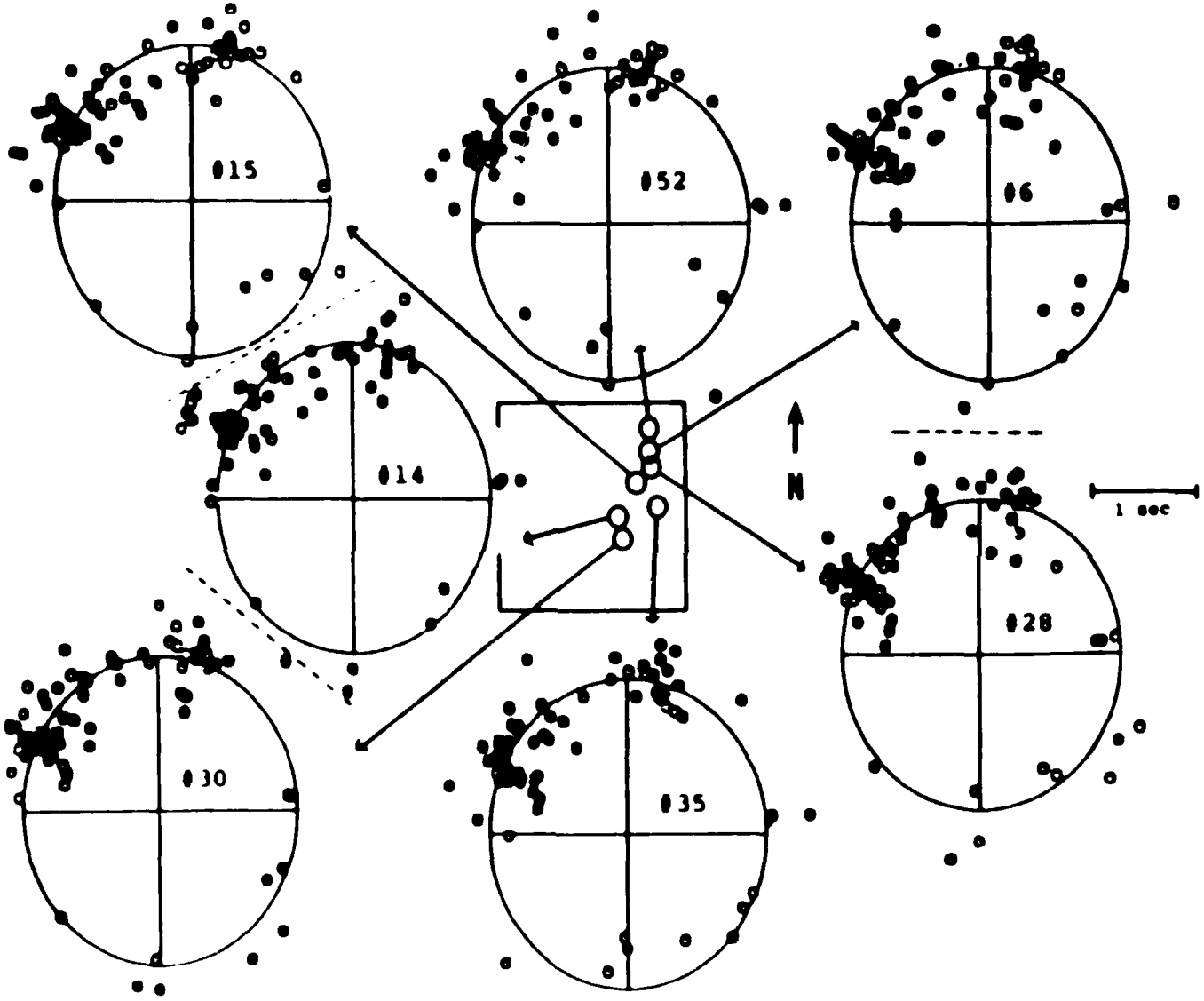

Figure 28. Azimuthal distribution of corrected travel time residuals as a function of event location; NE and central events. Circle represents zero residual; 1-second range is denoted.

example, Minster et al. (1981) found that m_b variations across NTS of the order of 0.4 magnitude units were accompanied by variations in the travel-time residuals of less than 0.4 seconds. Travel-time variations of this size are difficult to resolve from the rather imprecise times reported to ISC, particularly in view of the fact that the actual depths of the explosions at Shagan River are not known. In any case, it does appear that these P wave arrival time data will not be useful for identifying any variations in the subsurface geology across the Shagan River testing area.

IV. SUMMARY AND PRELIMINARY CONCLUSIONS

4.1 SUMMARY

The investigation summarized in this report has centered on a preliminary analysis of seismic variability at the Shagan River nuclear test site. Specifically, large samples of teleseismic P wave amplitude and arrival time data recorded from explosions at this test site have been collected and statistically analyzed in an attempt to define any systematic trends which correlate with source location.

The teleseismic P wave data base which has been assembled for this project was described in Section II where the distributions of the data with respect to source and station parameters were documented in detail. The data base is composed of individual m_b readings and P wave arrival times recorded by a selected network of 94 worldwide receiver stations from a sample of 52 Shagan River underground nuclear explosions which have been assigned m_b values of 5.5 or greater. These seismic data, together with the refined explosion epicenters and origin times determined by Marshall et al. (1984), constitute the data set which was used to investigate test site variability.

A systematic analysis of these data was described in Section III where the LSMF statistical analysis procedure was used to derive network-averaged event magnitudes and average m_b station correction factors for explosions at the Shagan River test site. The variations of these station correction factors with source location within the test site were then carefully analyzed and it was shown that large changes of the order of 0.5 units m_b can occur between relatively closely spaced explosions. Several alternate explanations of these m_b variations were then tested and critically evaluated through comparisons of data recorded at common

stations from selected pairs of explosions. This was followed by a preliminary analysis of the corresponding P wave arrival time data.

4.2 PRELIMINARY CONCLUSIONS

The analyses summarized above support the following preliminary conclusions regarding seismic variability at the Shagan River nuclear test site.

(1) Teleseismic m_b data provide strong evidence of systematic geophysical variations within the Shagan River testing area. In particular, corrected single station m_b residuals for explosions in the southwest portion of the test site appear to be random at any given azimuth and quite similar from event to event, while there are large (0.5 units m_b) variations in the corrected m_b residuals with azimuth between explosions in close proximity in the northeast and central portions of the test site.

(2) The observed azimuthal variability in the m_b station corrections with source location indicates that the network-averaged m_b values, and corresponding yield estimates, for explosions at Shagan River will be dependent on the specific azimuthal distribution of the stations used to compute the averages. This is an additional source of uncertainty to be considered in evaluating yield estimates determined from small network averages.

(3) The results of detailed comparisons of m_b residual data at common stations from selected pairs of explosions strongly suggest that the

observed variations in the azimuthal patterns of the m_b residuals are related to event location rather than tectonic release effects.

(4) Preliminary analyses indicate that the variations in m_b corrections for stations in a given azimuth are systematic enough that they can be contoured as a function of source location. This result supports the hypothesis that the observed differences are associated with changes in the near-source P wave propagation paths to teleseismic distances as a function of source location within the test site.

(5) In contrast to the m_b residual data, the reduced P wave travel-time residuals show no obvious correlation with event location. This is interpreted as an indication that the arrival time data reported to ISC is not precise enough to resolve the rather small travel-time variations which might be expected to accompany the observed m_b variations. In any case, it does not appear that the ISC travel time data will be useful for identifying variations in the subsurface geology across the Shagan River test site.

REFERENCES

Douglas, A., 1966, "A Special Purpose Least Squares Programme," AWRE Report No. 0-54/66, HMSO London.

Herrin, E., E. P. Arnold, B. A. Bolt, G. E. Clawson, E. R. Engdahl, H. W. Freedman, D. W. Gordon, A. L. Hales, J. L. Lobdell, O. Nuttli, C. Romney, J. Taggart, and W. Tucker, 1968, "1968 Seismological Tables for P Phases," Bull. Seism. Soc. Am., 58, 1193-1241.

Marshall, P. D., T. C. Bache, and R. C. Lilwall, 1984, "Body Wave Magnitudes and Locations of Soviet Underground Explosions at the Semipalatinsk Test Site," AWRE Report No. 0-16/84, HMSO London.

Minster, J. B., J. M. Savino, W. L. Rodi, T. H. Jordan, and J. F. Masso, 1981, "Three-Dimensional Velocity Structure of the Crust and Upper Mantle Beneath the Nevada Test Site," Systems, Science and Software Report to Advanced Research Projects Agency, SSS-R-81-5138.

North, R. G. and T. J. Fitch, 1981, "Surface Wave Generation by Underground Nuclear Explosions," Semiannual Technical Summary, March 31, No. ESD-TR-81-84 (Lincoln Laboratory, Mass. Inst. of Tech., Cambridge, Mass.), pp. 47-55.

Zlavdinov, L. Z., 1974, "Izucheniye stroyenia zemnoy kory po gravimetricheskii dannym" (Study of the Structure of the Earth's Crust from Gravity Data), Izd. Nauk, SSR, 119 p.

APPENDIX A

Station-corrected m_b residuals as a function of source location for events in central and northeastern Shagan recorded by all individual stations within the azimuthal window having an average of 3°. Stations denoted with (*) were used to compute mean residuals for contour plot in Figure 25. Shown here is the zero m_b residual contour line from Figure 25. Area displayed is 49.92 - 50.10 degrees North latitude by 78.90 - 79.05 degrees East longitude.

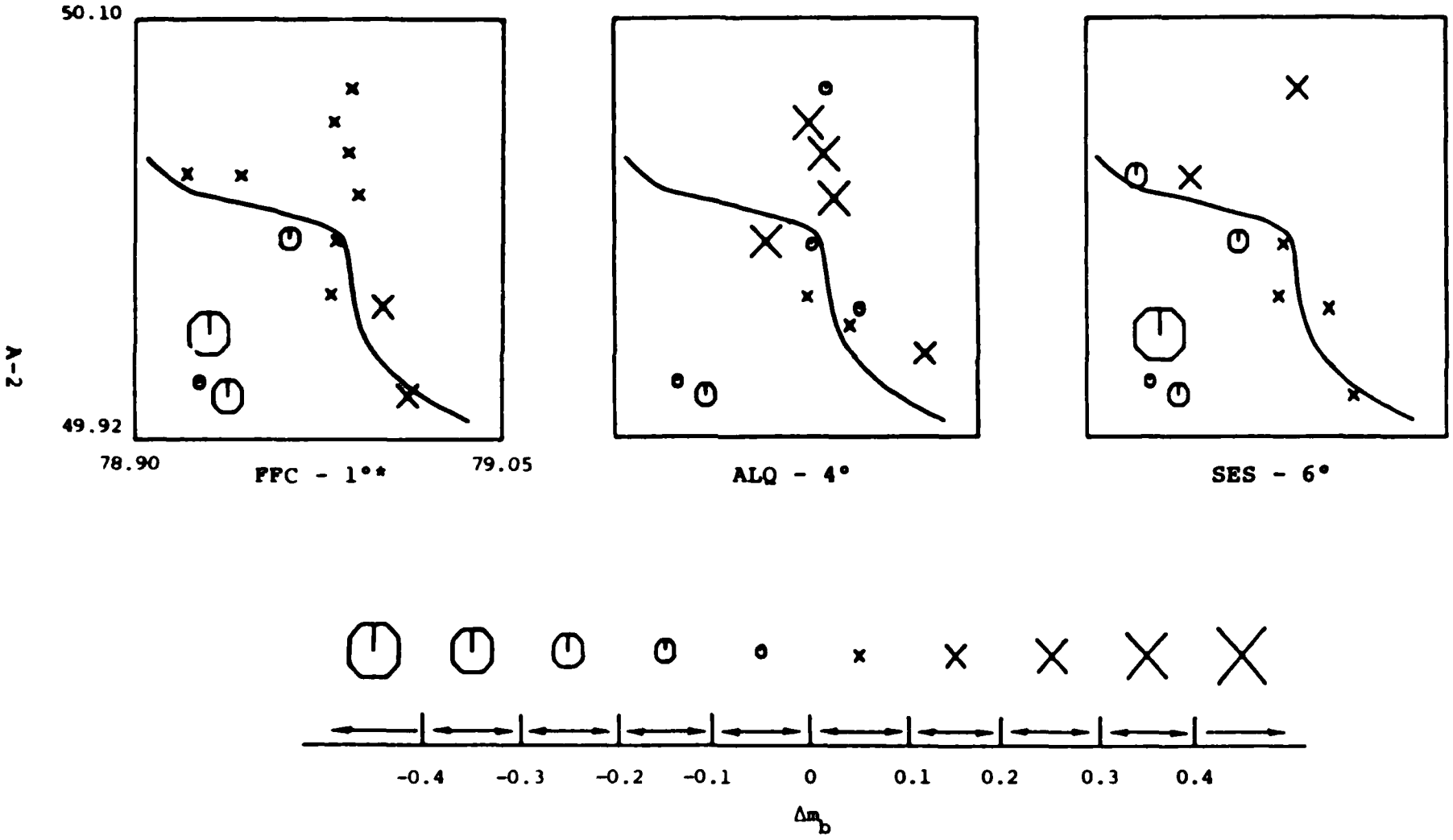

Figure A-1. Individual station-corrected m_b residuals as a function of source location.

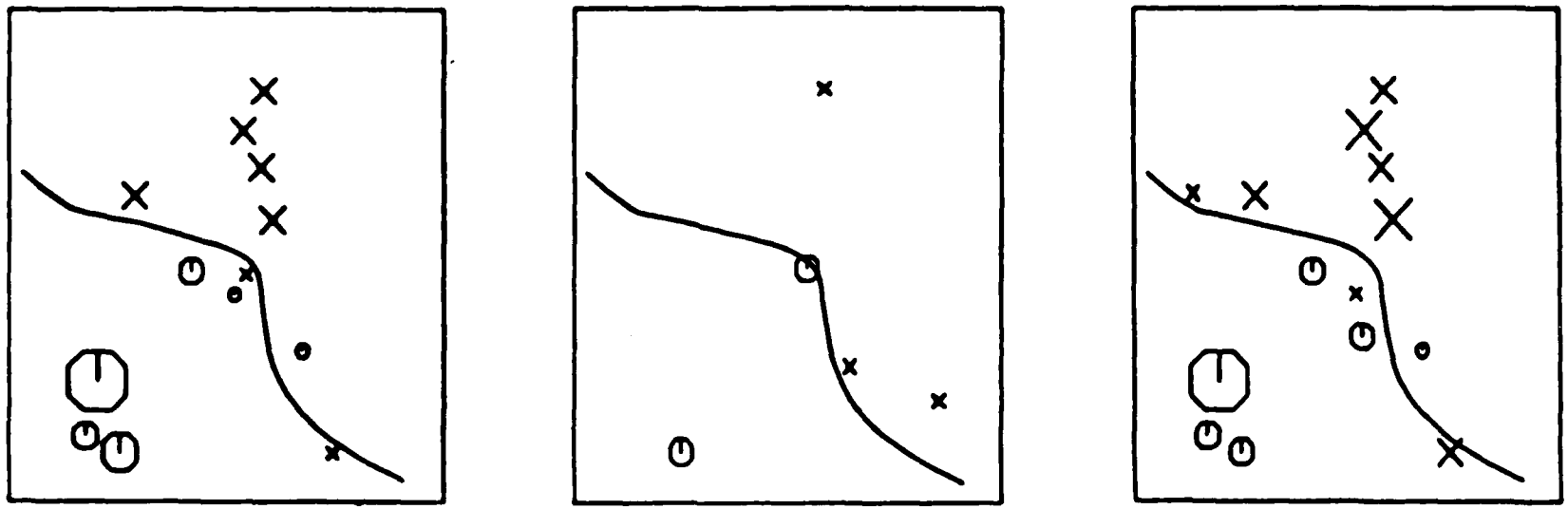

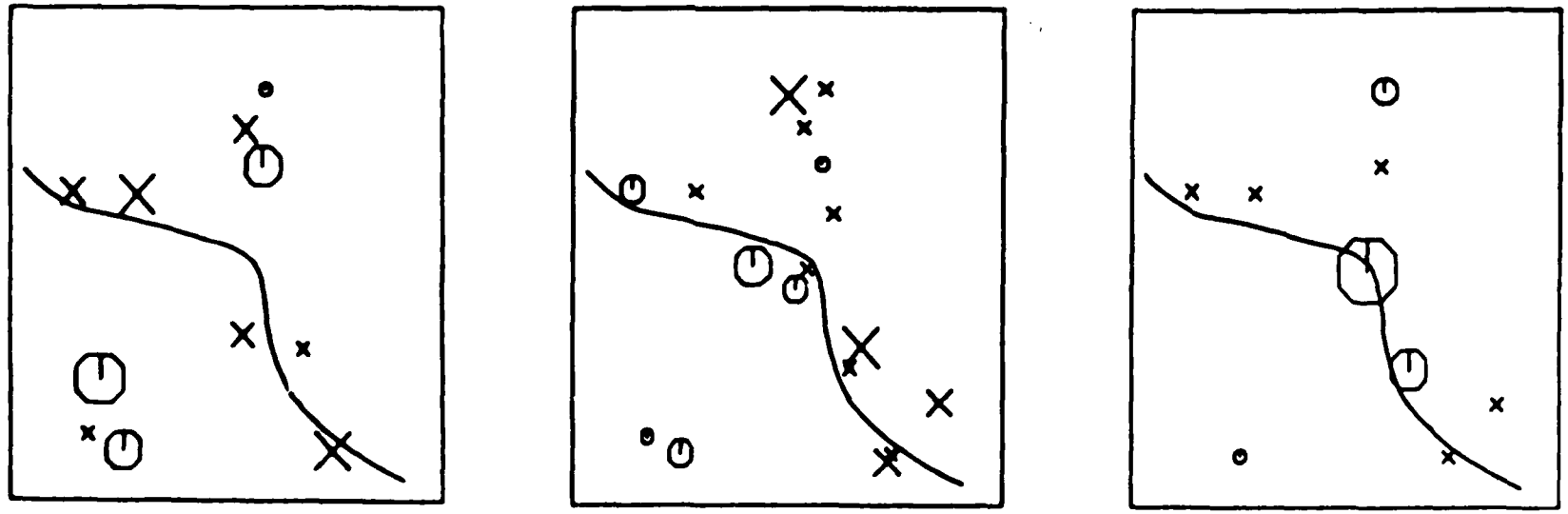

Figure A-2. *Individual station-corrected* m_b residuals as a function of source location.

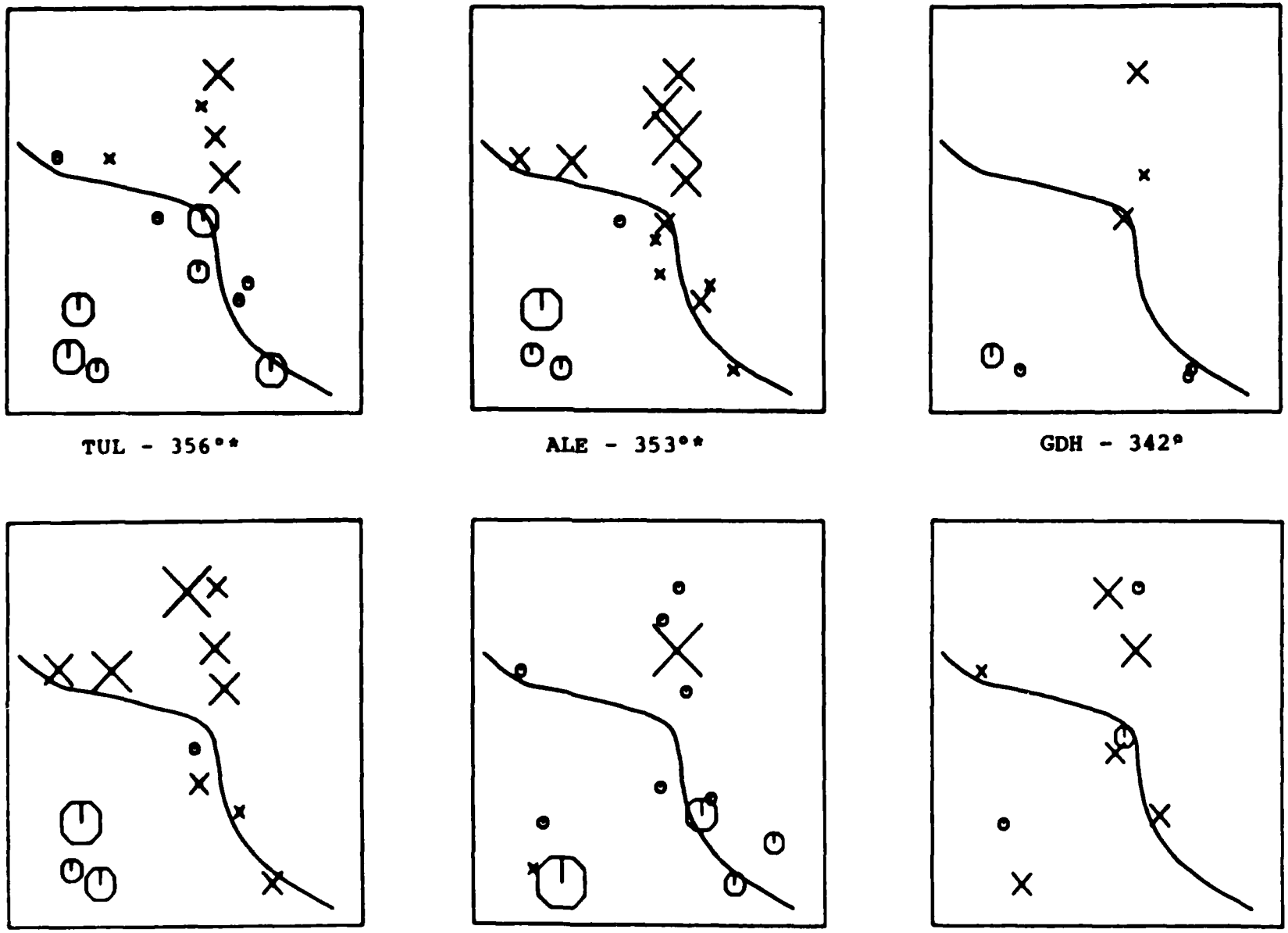

Figure A-3. Individual station-corrected m_b residuals as a function of source location.

END

9-87

DTIC